The Pandurra Formation, South Australia – An Integrated Assessment in 3D. Digital Data Release.

GEOSCIENCE AUSTRALIA

by

Bridgette Lewis

Australian Government
Geoscience Australia

Department of Resources, Energy and Tourism

Minister for Resources and Energy: The Hon. Gary Gray, AO MP

Secretary: Mr Blair Comley

Geoscience Australia

Chief Executive Officer: Dr Chris Pigram

GeoCat # 74075

Bibliographic reference: Lewis, B. (2012). The Pandurra Formation, South Australia. An Integrated Assessment in 3D. Digital Data Release.

Contents

Introduction

The Mesoproterozoic Pandurra Formation is a primarily coarse-grained, possibly fluvial sandstone within the Cariewerloo Basin that occurs within the central region of South Australia (Figure 1). The Pandurra Formation is strongly oxidised, and has a complex succession of secondary mineral overprinting in places. The proximity of the Pandurra Formation to mineral deposits such as Olympic Dam, the copper deposits located at the Pandurra Formation-Whyalla Sandstone contact around Pernatty Lagoon/Mt Gunson, and the now defunct Mt Whyalla barite mine has stimulated ongoing interest in assessing the Pandurra Formation for commercially viable mineralisation.

Study Rationale and Aims

This study is an assessment of the sedimentological and geochemical nature of the Pandurra Formation. It aims to update the existing state of knowledge by integrating comprehensive new field and drillhole core observations and geochemistry data with existing datasets to enable an integrated 3D assessment of the Pandurra Formation. Although prospectivity analysis is not the main aim of this study, special care has been taken to generate and release datasets which will enable this in the future. Specific aims are listed below:

- Compile existing Pandurra Formation and pertinent South Australian geological data and integrate this with new sedimentology and geochemistry data to present a complete data package in 3D.
- Assess the sedimentology, and in particular grain size, across the basin in order to improve knowledge of the evolution of the Pandurra Formation and how this can be utilised in understanding the prospectivity potential of the Cariewerloo Basin.
- Conduct a geochemical survey to complement the sedimentology aims and assist with future prospectivity assessment.
- Develop 3D methodologies including the interpolation of sedimentological and associated geochemical data and the ability to use these as predictive tools to allow integrated assessment of available datasets.
- Develop 3D and sedimentology/geochemistry methodologies with a view to enabling 4D fluid pathway assessment of the Cariewerloo Basin and other sedimentary basins in the future.

This document is intended to provide the methodological background for the data release including the field, geochemical, and 3D methodologies along with some comment on the success and limitations of the approach used, and some example images of the types of GOCAD objects generated. The full digital structure of the release is recorded in the ‘File_Structure_Digital_Release.xlsx’ file.

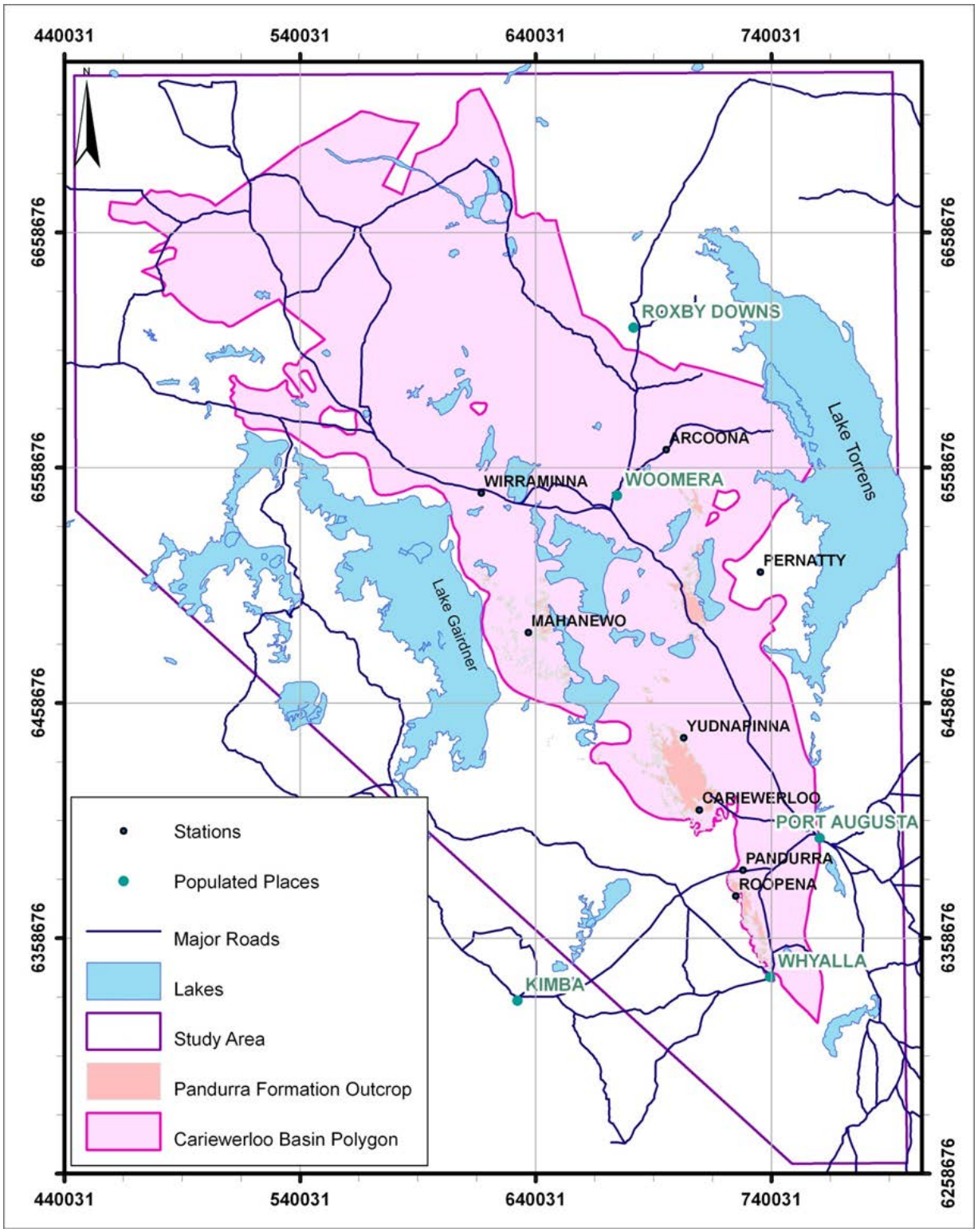

Figure 1: *Map showing location of Study Area (purple), Cariewerloo Basin Polygon (pink), outcropping Pandurra Formation (rose pink), Major roads (blue line), and lakes (blue infilled polygons). Selected populated places and homesteads are also shown.*

Spatial Extent and Datum

All data for this report are projected in GDA94 Zone 53. While the study area occurs in both Zone 53 and Zone 54, the tiny proportion of the area in Zone 54 was deemed insufficient to warrant using a projection system designed for very large spatial extents. All GOCAD files are in Eastings and Northings, where externally acquired data has additional latitude/longitude information available this has also been included. All 'z' or elevation values are given relative to the GOCAD interpolated DEM unless explicitly stated otherwise (e.g. GPS elevations), or for artificially generated trend lines (e.g. Eastern_Trendline_Geochemical_Trendline.pl). The approximate area covered in this study is given below. The voxet area is slightly less than the area covered by the Study Area Polygon to reduce GOCAD processing time, and ease voxet generation by using a regular shaped voxet boundary.

Table 1: Spatial Extent of this study.

Projected Map Extent of Study Area			Projected Map Extent of Voxet		
	Easting	Northing		Easting	Northing
SW Corner	444,200	6,263,000	SW Corner	445,000	6,305,000
NE Corner	791,409	6,726,000	NE Corner	765,000	6,725,000
				Upper Limit	Lower Limit
			Depth (m)	1000	1400

File Structure

The basic file structure of this data release is a follows:

- Digital Release Readme
- File Structure Digital Release
- Underlying Data
  - Field Data
  - Geochemistry
  - Reference
  - Well Data
  - Summary_Data.xls
- GOCAD Objects
  - Cartographic
  - Classifications
  - Field Data
  - Geochemistry
  - Geology
  - Physical Characterisation
  - Reference Datasets
  - Well Data

Comment on the content of the data release, datasets used, references and acknowledgements, etc. will now be discussed using the same structure as above. A note of caution is issued with regard to the Pandurra Formation well intersections. During the course of this study, a number of wells were assessed for possible extensions to the known Pandurra Formation extent based on preliminary sedimentological and geochemical data. The wells that may have modelled preliminary interpreted Pandurra Formation extensions in the 3D model are shown in Table 2. These interpretations are only preliminary, and should be used with caution. The original well intersections can be found in the summary data spreadsheets of this study; the primary information source is DMITRE's online interface SARIG (https://sarig.pir.sa.gov.au/Map).

Table 2: Summary of drillhole sections and outcrop localities outside the currently accepted limit of the Pandurra Formation assessed in this study. Drillholes located 'outside basin margin' status is relative to the Cariewerloo Basin polygon used this study.

Drillhole Extensions	Formal Name	Informal Name	Measured depth top (m)	Measured depth base (m)	Notes	Geochemistry Status
	6699	BDH2	285	290.35	Sediments below base of Pandurra. GRV sediments?	Not analysed
	139595	PSC7/SASC3	695.3	696	Altered Pandurra sediments below highly altered dyke?	Not analysed
	165607	SAE 4	784.5	1140	Highly blue-black altered Pandurra below accepted base?	Not analysed
	165606	SAE 3	752	764.2	Highly blue-black altered Pandurra below accepted base?	Not analysed
	25359	WHD 1	631.98	683.53	Blue-black altered Pandurra below accepted base?	Not analysed
	139594	PSC4/SASC2	271.39	298.4	Sediments above Pandurra - maybe Whyalla Sandstone?	Analysed. Not included in Pandurra Geochemistry this study
Drillholes Outside Basin	9605	ERD 6	102	104	Outside basin margin, not accepted as Pandurra	Analysed. Not included in Pandurra Geochemistry this study
	9607	ERD 8	68	69.33	Outside basin margin, not accepted as Pandurra	Analysed. Not included in Pandurra Geochemistry this study
	9608	ERD 9	23	24.3	Outside basin margin, not accepted as Pandurra	Not analysed
	20831	BLD 2	646.6	696.7	Outside basin margin, typically accepted as Pandurra	Analysed. Included in Pandurra Geochemistry this study
	25360	SLT 101	1379.5	1391.3	Outside basin margin, typically accepted as Pandurra	Analysed. Included in Pandurra Geochemistry this study
	29739	Wokurna DDH6	118.3	329	Outside basin margin, not accepted as Pandurra	Analysed. Not included in Pandurra Geochemistry this study
	104376	BUMBARLOW1	408.95	720.33	Outside basin margin, not accepted as Pandurra	Analysed. Not included in Pandurra Geochemistry this study
	205821	CAR001	426.9	541	Just within eastern basin margin, no Pandurra logged	Not analysed
	205822	CAR002	422.9	556	Just within eastern basin margin, no Pandurra logged	Not analysed
	209917	RC-DD04TI008	621.75	797.8	Drillhole outside basin, typically accepted as Pandurra	Analysed. Included in Pandurra Geochemistry this study
	25357	SLT 107	735.8	809.3	Outside basin margin, typically accepted as Pandurra	Analysed. Included in Pandurra Geochemistry this study
	25356	BDH3	1116.2	1124.8	Just outside basin margin, not accepted as Pandurra	Analysed. Included in Pandurra Geochemistry this study
Outcrop	Pandurra09_31	Wirraminna Salt Lake S4			Outside basin margin, not accepted as Pandurra	Analysed. Included in Pandurra Geochemistry this study
	Pandurra09_28	Wirraminna Sth-Mahenewo White Cliffs			Drillhole outside Pandurra polygons	Analysed. Included in Pandurra Geochemistry this study

Data

Underlying Data

The underlying data files constitute all the underpinning data used in this study in its original pre-GOCAD object format that is being digitally released. The 'Summary_Data.xls' file sitting at the topmost level of these folders summarises many of the field and well observations underlying the physical characteristics of the GOCAD objects. The other folders contain the original data in (primarily) Excel formats for ease of end-user manipulation. Of particular note is the ICPMS geochemistry data, which complements the XRF data, but was largely unavailable for use during this study. It can be widely used for other purposes, and that is why it has been included here.

Data Attribution for Underlying Datasets:

A summary table of datasets used in the production of this study can be found below in Table 3. All data from SARIG have been downloaded in their original form and where appropriate reproduced in that original or derivative form in accordance with DMITRE's licensing and permission. As many datasets have been modified during the course of this study, it is strongly recommended that if users want to use the original datasets they download them from SARIG (https://sarig.pir.sa.gov.au/Map) to ensure they are using the most recent and unmodified version of the data. Hylogger data is produced with Federal Government NCRIS funding administered by Auscope, and is produced using technology with trademarked intellectual property held by CSIRO (HyLogger™ and TSG™). In the Structural_Data sub-folder, field observations from the author are supplemented by those kindly provided by Wayne Cowley and Tania Wilson (DMITRE).

Table 3: Published datasets used in this assessment

Category	Dataset	Reference	Subsidiary Datasets/Notes
Cartographic	SRTM Derived 1 Second DEM version 1.0	Gallant, 2011	
	Google Earth Satellite Imagery	Google Earth 2009	Used for initial field work phase only
Geology	1:100,000 geology polygons (State_MGA)	SARIG, 2009	
	1:50,000 geological map images	Cooper and McGeough, 2006	1:50,000 map images covering the Cariewerloo Basin. Used for initial field work phase only
	DH_Strat well Database	SARIG, 2011	
	Mindep Database	SARIG, 2011	
	Hylogger spectra	SARIG	
	Cariewerloo Basin DVD GOCAD files	Wilson *et al*., 2011	Faults, Member Surfaces, Pandurra Formation Surfaces
Geophysics	Gravity	Bacchin *et al*., 2008	
	Radiometrics vs 2.0	Minty *et al*., 2010	
	Magnetics, Magmap vs 5.0	Milligan *et al*., 2010	
Reports	Company Reports	SARIG, 2009	Compiled for end-user ease of use in Reference folder

GOCAD Objects

GOCAD objects have been released separately as objects, instead of as pre-loaded project files to ensure compatibility with any version of GOCAD. These files have been generated primarily with GOCAD 2009.1. All 'artificial' GOCAD curves generated (Region curves, geochemical trend lines etc.) sit in 3D space at a constant Z value (often Z=0), this can easily be changed by modifying the Z value to force the curves to sit above an exaggerated DEM, or other features as required. A note on the location of the Bumbarlow1 well (DH104376). This well's spatial location was recognised to be incorrect after the completion of the model. The location of the well and all its derivative datasets including geochemistry, physical characteristics etc. have been relocated. This has not impacted on the surfaces in the model as this well is located significantly outside the Cariewerloo Basin margin. While every effort has been made to change all Bumbarlow1 spatial references, the possibility of spatial location error is greater for this well.

Cartographic

These datasets delineate the study area, the modified and original Cariewerloo Basin Polygon, the final DEM surface in various forms, and the Pandurra Formation thickness trend lines (Depocentres). Location of field and well locations, and the location of mines and deposits within the study area are also included.

Classifications

These are the files that enforce particular colour ramps on various GOCAD objects generated this study. These need to be loaded into GOCAD before any other objects to ensure the correct display of many properties. Particular important is the Grain_Size.xml which controls the appearance of the voxet property – Grainsize_Classified.

Physical Characterisation

These files are the summary GOCAD point files of many of the physical sedimentological observations made during the core logging and field work phases of this study. These files include parameters such brecciation, conglomerate, Gairdner Dyke localities (observed this study, not from SARIG) etc. Many of these files, in particular the files associated with characterising Pandurra Formation alteration require classification file loading to enable correct viewing.

Field Data

The field data files summarise the grain size transects used during the interpolation of the grain size voxet property as generated from field observations. The field sites as formally numbered individual localities, the gamma logged field transects, and the structural and paleoenvironment measurements recorded during this study and as provided by W. Cowley (Cowley_Structural_Measurements.vs).

Geochemistry

The location of geochemistry and thin section samples, and the original XRF and ICPMS data as points are included here. The PIMA data used in this study is included as both locations of individual minerals and as Mica Crystallinity, Mica Abundance, and Mica Wavelength files. The PIMA data harv been resampled to 1.0 m averages to reduce processing load. The primarily geochemistry derived trend lines generated during the course of study (Northwest Fault, Ridgeline West, Ridgeline East, and Eastern Trendlines), at the surface of the voxet are also included here.

Geology

This folder contains the majority of the final interpolated products used to assess the Pandurra Formation in the Report and the objects used to make those products. The draped simplified geology polygons used to generate each geological surface, and an example of the constraints used to generate those surfaces are provided for the Upper Pandurra Formation surface. The final geological surfaces generated this study and the features used to define the voxet extent, are also included here.

The final geological and geophysical voxets sit within this folder; these host the final interpolated grain size, geochemistry, and spatial products of this study. Voxet properties are too numerous to list here, but cover the classified and unclassified grain size, individual geochemical species from the XRF data as oxides, elements, and the iron and Na/Al ratio, and spatial 'distance to' voxet properties. The distance to voxet properties are the calculated distance from the faults used this study, from the basal surface of the Pandurra Formation, from other fault datasets, draped geological polygons etc. These can be used to spatially query the geochemistry or grain size properties to enable higher level assessment for exploration etc. e.g. 'distance from Fault X where U>5 ppm. The ten grain size isosurfaces generated are also included here; these represent curves of constant grain size and are derived from the Grainsize_DSI voxet property. These provide a simple way of spatially showing grain size distribution without having to slice the voxet. The isosurfaces need to be viewed together to create closed volumes, otherwise they appear as open curves.

A note on displaying the voxets:

The voxets are very graphic intensive, if the voxet does not display on first loading, try changing one of the voxet attributes e.g. Display the cage, then hit the refresh screen (globe) button at right of screen. This forces the program to graphically refresh, and should result in the voxet displaying on the screen.

Reference Datasets

The faults used in this study are largely derived from DMITRE (formerly PIRSA) 3D objects. Also used for reference purposes are the Pandurra Surfaces, AEM surfaces and curves, Member Subdivision datasets, and Hylogger interpreted surfaces. These datasets are from the PIRSA Cariewerloo Basin Unconformity-Related Uranium Project (2011). They have been used and are reproduced here under the Creative Commons 3.0 license. The full reference for the datasets is as follows:

Wilson, T., Bosman, S., Heath, P., Gouthas, G., Cowley, W., Mauger, A., Gordon, G., Baker, A., Dhu, T., Fairclough, M., Delaney, G., Roach, I., Huchison, D. and Costelloe, M. 2011. Cariewerloo Basin Unconformity-Related Uranium Project: Data Release April 2011. Geological Survey of South Australia, Department for Manufacturing, Innovation, Trade, Resources and Energy (formerly Primary Industries and Resources SA). DVD.

Well Data

The well data folder contains all the grain size data generated this study as well as the well markers derived from the SARIG database and simplified this study to build the geological surfaces. The data are presented in a variety of formats for ease of viewing. The grain size data are presented as logged individual wells and as a well group. The grain size data are also included as a series of point files that represent various re-samplings of the original 1 cm logged grain size curves as recorded in the .xls and .csv logs in the Data-Well Data-Grainsize Logs section of the data release. The grain size logs used in the final interpolation of the Grainsize voxet property are those in the Grain-Size_Upscale_01m_mean.vs file. These are also the points displayed as grainsize logs associated with the wells GOCAD objects.

The wells used to generate the geological surfaces are also presented as individual wells and as a well group. In addition, they are presented as the ‘Well Markers Tops’ and ‘Well Markers Modified for Modelling’ well marker point files. The modified well markers have been altered to enable geological surface modelling – they do not exactly match the simplified well geology seen in the ‘All_wells_simplified_geology.csv’ file (see Report method for clarification).

Methodology

Site Selection

Field sites were pre-selected using 1:50,000 geology maps, company data, aerial photography, and satellite imagery. Once in the field, a seven day reconnaissance trip was used to evaluate preselected sites prior to detailed logging. Forty-eight sites were logged in detail to document sedimentary structure, structure (including strike/dips), grain size, sorting, grain angularity, composition, paleocurrent direction, alteration, brecciation etc. Seventy-three field samples were collected during this period for geochemistry, of these 61 were processed for geochemistry for this report. Summary Table 4 details field sites assessed, Figure 3 shows the location of field sites together with wells and reconnaissance sites. Field work observations are summarised in the workbook 'Summary_Data.xls, the same basic methodology was applied to the field grain size observations as for the drillhole grain size data (see later).

Table 4: Field Site summary table showing formal site number, descriptive site name, and GPS location. The Z value (m) given is not a GPS reading, but is derived from the GOCAD rendered Digital Elevation Model (DEM) surface for consistency.

Site Number	Site Description	GPS E	GPS N	DEM Z
Pandurra09_11	Cariewerloo	712180	6417547	226.85
Pandurra09_18	Conglomerate Hill	703029	6409481	228.86
Pandurra09_18A	Conglomerate Hill	703264	6409497	211.48
Pandurra09_34	Emmie Bluff Arcoona station in situ P hunt 1	703783	6547716	168.85
Pandurra09_36	Emmie Bluff Arcoona station in situ P hunt 2	707221	6550230	122.35
Pandurra09_37	Emmie Bluff Arcoona station in situ P hunt 3	707130	6548612	103.24
Pandurra09_38	Emmie Bluff Arcoona station in situ P hunt 4	708311	6543325	98.69
Pandurra09_17	Gap Dam	704057	6410333	194.24
Pandurra09_16	Gap Dam	704063	6410206	196.51
Pandurra09_15A	Gunters Gorge creek traverse - bottom of gorge	714732	6415808	192.93
Pandurra09_15	Gunters Gorge creek traverse - middle of gorge	714609	6416032	213.69
Pandurra09_14	Gunters Gorge creek traverse - top of gorge	714444	6416409	230.08
Pandurra09_13	Gunters Gorge Bluff	714443	6416412	229.42
Pandurra09_23	Hotel Creek	704546	6431108	194.61
Pandurra09_22	Hotel Creek	704693	6431180	192.86
Pandurra09_33	Mahenewo mesa hunt mesa 1	643188	6490043	121.51
Pandurra09_32	Mahenewo mesa hunt mesa 3	645967	6491049	101.50
Pandurra09_39	Mt Gunson Mine	704034	6519455	81.97
Pandurra09_04	Mt Laura	735792	6346238	140.95
Pandurra09_05	Mt Whyalla	728770	6364642	115.81
Pandurra09_06	Mt Whyalla - big pebbles site	728020	6365874	187.43
Pandurra09_07	Mt Whyalla 2	728121	6365727	189.21

Site Number	Site Description	GPS E	GPS N	DEM Z
Pandurra09_45	Pernatty station under the transmission lines	708700	6499019	98.67
Pandurra09_41	Pernatty station under the transmission lines - S1	706302	6503607	99.67
Pandurra09_42	Pernatty station under the transmission lines - S2	706478	6503375	100.20
Pandurra09_40	Pernatty station under the transmission lines - S3	706840	6503378	92.88
Pandurra09_44	Pernatty station under the transmission lines - S4	708446	6498824	95.31
Pandurra09_19	Poutchina Hill Traverse	707656	6412328	213.02
Pandurra09_20	Poutchina Hill Traverse	707755	6412553	234.50
Pandurra09_01	Railway cutting Whyalla	738673	6343906	26.53
Pandurra09_10	Red Rock	727840	6376035	106.11
Pandurra09_08	Roopena Creek bed 1	728765	6371974	138.53
Pandurra09_08A	Roopena Creek bed 2	728437	6372021	138.72
Pandurra09_09	Roopena Creek bed 3	728322	6372170	145.43
Pandurra09_21	The great silt hunt	706234	6419658	216.14
Pandurra09_03	Water tank hill Whyalla - Moonabie transition	738636	6343353	25.10
Pandurra09_02	Water tank hill Whyalla- Quarry	738606	6343451	25.07
Pandurra09_29	Waynes 'granite' contact	628753	6507985	117.86
Pandurra09_43	Waynes railway cutting	710046	6489968	71.78
Pandurra09_30	Wirraminna salt lake Section 1	620535	6511445	128.74
Pandurra09_30A	Wirraminna salt lake Section 2?	620490	6511543	128.89
Pandurra09_30B	Wirraminna salt lake Section 3?	620522	6511615	128.80
Pandurra09_31	Wirraminna salt lake Section 4	602583	6511652	121.44
Pandurra09_28	Wirraminna Sth - Mahenewo drive: white cliffs	628887	6507996	118.00
Pandurra09_24	Yudnapinna - woolshed creek	695692	6439692	215.69
Pandurra09_26	Yundapinna creek traverse 3	699938	6443264	181.15
Pandurra09_27	Yundapinna creek traverse 2	699963	6443291	179.79
Pandurra09_25	Yundapinna creek traverse 1	700140	6443295	174.41

Field grain size observations were digitally recorded as transects and points. Transects are used where gamma logging has provided a start and end GPS point for each section. These are used to plot the transect lines – first in ArcGIS to generate the line, which is then turned into a series of xyz points in GOCAD. These points are then attributed with grain size values based on field observations. The field reconnaissance points were also attributed with grain size values to provide supplementary points. All field data Z values are derived from the GOCAD interpolated 1 second Digital Elevation Model (DEM) (Gallant, 2011).

Drillhole Data Methodology

Sample Acquisition

Drillholes selected for analysis were chosen from the DMITRE drillhole database hosted by SARIG on the basis of the availability of diamond cored material from the Pandurra Formation held at Glenside Core Library. This search yielded 147 drillholes. This number was reduced by evaluating 3D spatial location of drillholes, portion of Pandurra Formation penetrated, proximity of other drillholes, representative lithology, and proximal/distal relationship to sediment and mineralisation sources e.g. basin margins and known mineralised deposits. In total 67 drillholes were inspected at Glenside Core Library during August-September 2009. During this period, core was assessed for sedimentary structure, grain size, sorting, grain angularity, composition, alteration, brecciation, volcanic intrusion presence etc. Representative sampling of cores for geochemistry analysis was completed during the same period, and attempted to capture the full spectrum of lithological variation. A full summary of drillholes inspected and sampled can be found in the Summary_Data.xls spreadsheet. Figure 3 below shows the spatial distribution of both drillholes and field sites inspected for this report.

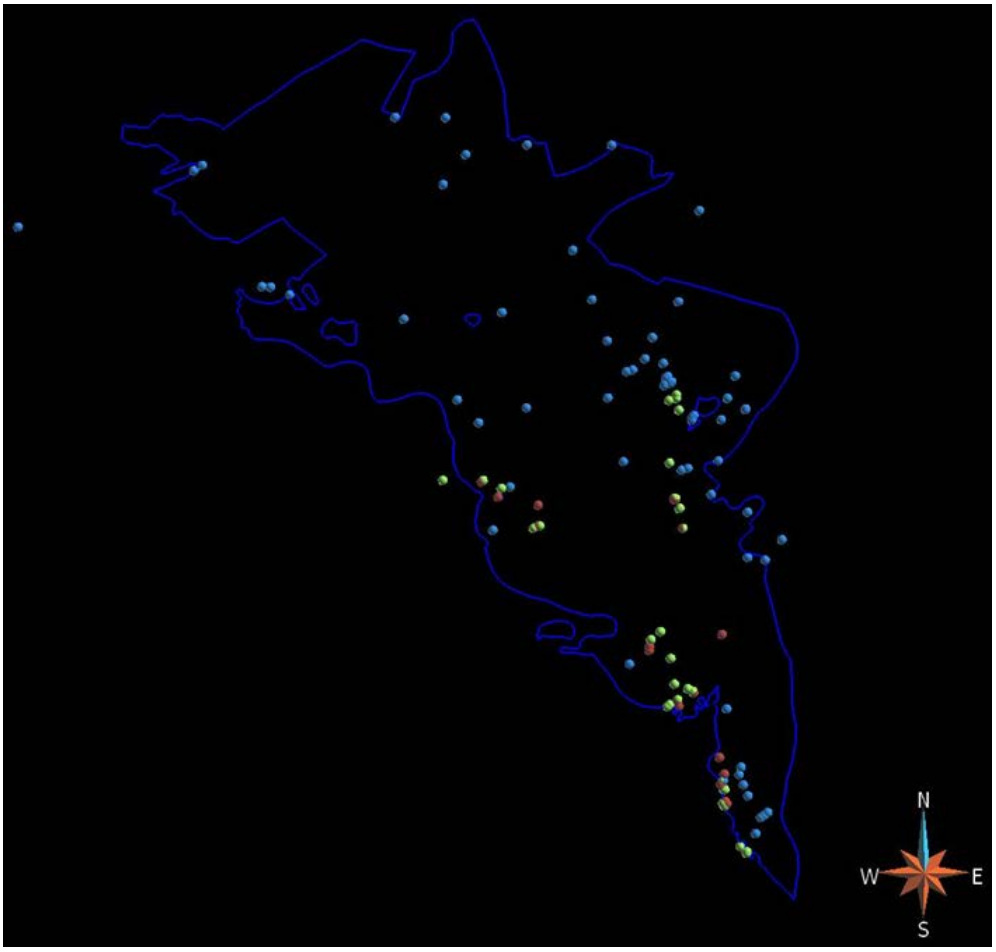

Figure 3: *Location of logged drillholes used in this study (blue) with field sites (pale green), reconnaissance field sites (red), and Cariewerloo Basin Polygon Modified (blue curve) shown for reference. Plan View.*

‘Average’ Grain Size Curve Generation

The grain size curves used in this study record the ‘average’ grain size of the Pandurra Formation at a resolution of 1 cm. Average grain size curves were generated as an alternative to the traditionally laboriously hand-drawn logs of grain size and matrix proportion (and subsequent digitised curves) to simplify the process of digital log generation, while still capturing the total grain size variation. These logs are representative of the variation occurring in any given core interval, but do not exactly represent the centimetre by centimetre true physical variation of the core – rather they capture the numeric variation in grain size within an interval.

At the time of inspection, grain size and matrix information was recorded in detail for each core interval. Intervals were of varying thickness dependent on the degree of variation in lithology; the more variation present, the shorter the logged intervals. These descriptions assess bed and cycle thickness, cyclicity and style of sedimentary structure, grading, colour, grain size variation, and matrix proportion etc. within an interval. They do not record exact measured depths for every centimetre of observation. The raw textual descriptions do capture significant variations in grain size as exact measured depths – examples of these observations include first appearance of shales and major shale intervals, maximum grain size beds (termed pebble maximums), major pebble conglomerates, dykes, and alteration horizons. On completion of the textual logging, these descriptions were digitally captured and rendered into grain size curves. The grain size classification system used is a simplification of the Wentworth Scale (Wentworth, 1922) and is shown below in Table 5. All sediments with a grain size smaller than 0.063 mm (<4φ) have been termed ‘silt’ in this report, the exception being highly altered clay rich intervals which have been systematically logged as .040 mm (8φ) to differentiate these intervals in the final logs. The formal terminology around pebbles, cobbles, and boulders was also slightly modified to better represent the grain size variation found in the Pandurra Formation. During the process of recording the core observations, the use of the term ‘pebbles’ was liberally applied, but measured diameters recorded within the textual descriptions are reliable and this is what has been used to generate the grain size curves. While descriptions of the stratigraphy above and below the Pandurra Formation have been recorded textually (where available), only the Pandurra Formation was numerically logged. Gairdner Dykes or other unidentified intrusive units are recorded in the textual logs, and appear as a ‘no data’ value (-9999) in the numeric logs.

Table 5: Modified Wentworth Scale used for grain size classification used in this report.

	Lower (mm)	Upper (mm)
alteration/clays	0.04	0.04
silt	0.05	0.063
very fine sand	0.063	0.125
fine sand	0.125	0.25
medium sand	0.25	0.5
coarse sand	0.5	1
very coarse sand	1	2
granules	2	4
pebbles	4	16
cobbles	16	64
boulders	64	256

Grain size curves were generated in Excel at a resolution of 1 cm, and the final versions of the core logging and digital grain size curve data can be found in the digital appendices folder ‘Grainsize_Logs’. These files

include the textual logging, the digital data underlying the grain size curves, and the plotted grain size curves (as Excel workbooks for each logged drillhole), as well as the final .csv files used for GOCAD loading.

Ideally, four numeric grain size curves would have been generated for each core section – one with matrix size and another with matrix percentage, a third with clastic grain size and the last with clastic percentage. These could then be combined to give an accurate overall indication of grain size. However, due to time constraints, an intermediate approach where these characteristics are evaluated and incorporated into one curve has been adopted as follows. In order to create a representative grain size curve, the proportion of matrix has been taken into account in the overall grain size. Thus an interval where pebbles are 20 mm and matrix is 20% will yield a slightly different grain size result than a section where pebbles are 20 mm and matrix is 50%. For many intervals this process makes little observable difference to the final numeric output as the matrix contents are generally quite low. Only where dramatic matrix proportion variations occur does this approach become noticeable. This approach should give a good representation of grain size variation, while cutting down logging time significantly.

While generating the grain size curves this way has a number of advantages, there are also some limitations. Most importantly - these curves cannot be used as direct high-resolution references to core (though the textual observations can). They also do not look as smooth as hand drawn curves when inspected closely. With all the inherent natural variation in gradation, and given that every gradation requires a unique mathematical equation to represent it, generating naturally curved numeric grain size curves is not feasible. Thus in this study, grading is usually represented as a linear transition from one grain size to another. A particularly common scenario that has been accounted for in a more curvilinear fashion is the gradual grain size transition from very fine to coarse sand, then an abrupt grade into pebbles. This has been generated using a line with two different slope functions. Very occasionally, where gradational curvature has been particularly desirable, the time has been taken to generate a natural looking curve between the two end members using a numeric curve function.

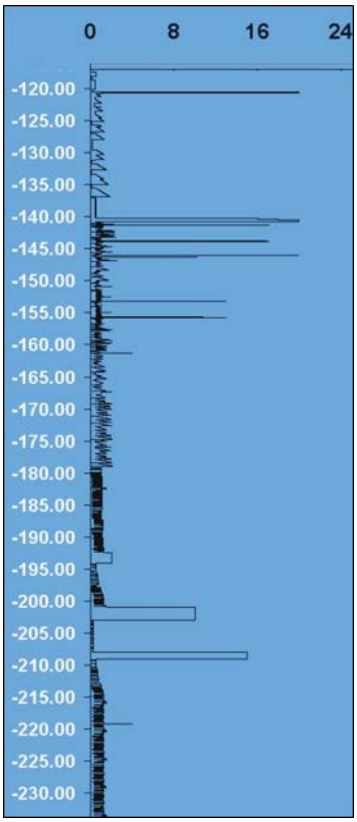

Figure 4: *Example grainsize log from PY1 (DH 20712) with grainsize in millimetres on the x axis and depth in metres on the y axis. Graded beds as treated numerically in this study are visible from 120 – 135 m in particular; coarser grained beds exhibiting the 'stepped' character referred to in text also visible.*

In addition to generating grain size logs and textual data, a series of summary sedimentology datasets were also compiled. Significant sedimentological features were extracted and recorded as individual datasets to aid in interpretation - these are: First Shale, Shale Zones, Heavy Mineral Banding, Angularity, Pebble Maximums (depth and size range), and Top and Basal Conglomerates. All of these are found as individual features in the Final_Summary.xls spreadsheet and as GOCAD objects in the digital appendices.

In addition to the sedimentology datasets, the structural/geochemical datasets 'Brecciation', 'Dykes', 'Major_Alteration', and 'Other_Alteration' were generated. 'Brecciation' is a summary of the significant brecciation observed in the field and in drillcore. Only true brecciation was recorded in this dataset – areas of pervasive faulting are reflected in the 'Fault' datasets. The 'Dykes' dataset is drawn from the drillhole observations for this study where Gairdner Dolerite dykes have been directly observed in the process of drillhole logging. Dykes recognised in SARIG are also included as a separate GOCAD objects (e.g. PIRSA_Gairdner_Dykes_Markers_Tops). 'Major_Alteration' encompasses the significant and/or pervasive blue-black, cuprous, black cement, anhydrite, and clays alteration horizons. The 'Other_Alteration' dataset records all alteration as both abundance in sample, and as pure alteration type by location. Sixteen major styles of alteration were recorded. The compilation of these additional datasets enables spatial evaluation of the complex alteration overprinting seen in the Pandurra Formation. All of these datasets were loaded into GOCAD as point sets with classification (.xml) files as necessary and can be found in the digital appendices.

Geochemistry Methodology

Sample Selection

Two hundred and ninety five samples were taken during the core library and field work phases of this study. Given time and processing limitations, the sample population was assessed for the following characteristics: 3D location, lithology, pre-existing Pandurra Formation member subdivision based on Tonkin (1978) and Mason (1980), weathering, potentially economic mineralisation, and proximity to known deposits. After these characteristics had been evaluated, 207 samples were chosen for analysis, of which 146 were core samples and 61 were field samples.

All geochemistry samples were photographed and described in detail during the process of sample preparation. The sample descriptions can be found in the digital appendices. Geochemistry sample locations are shown in Figure 5 and data can be found in Excel formats in the Underlying Data -> Geochemistry folder.

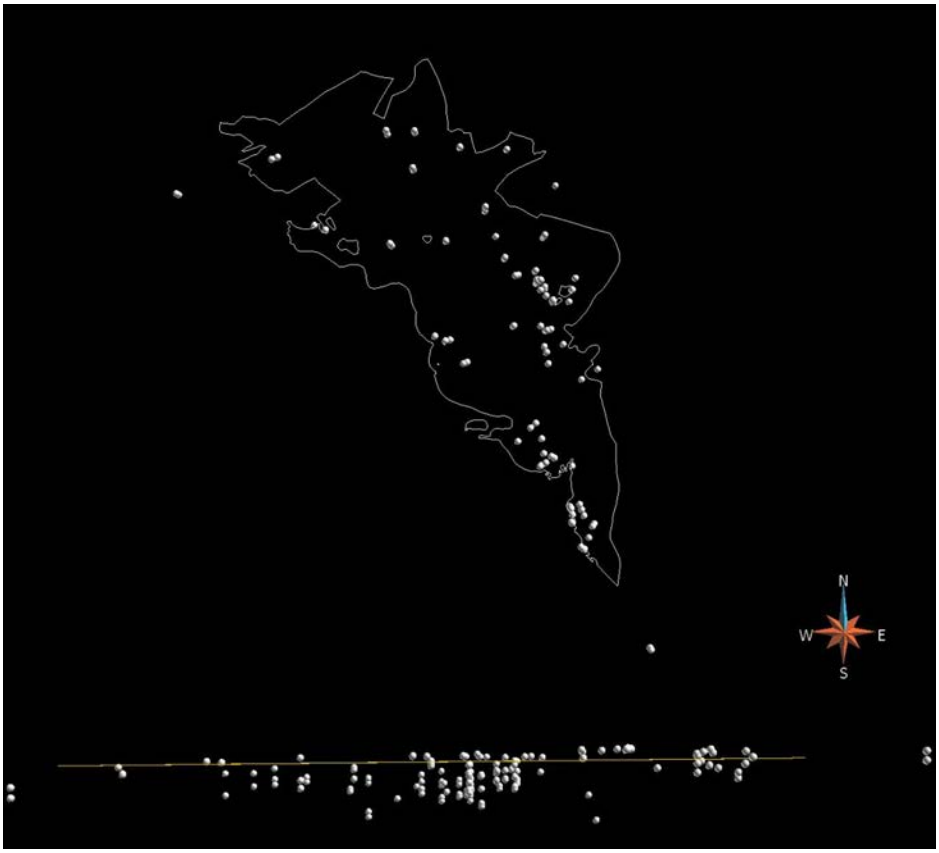

Figure 5: *Location of geochemistry samples in plan (upper) and side on views (lower). Side on view is looking NE across the long axis of the basin, vertical exaggeration approximately 20 x. Cariewerloo Basin Polygon Modified shown for reference (white curve).*

XRF and ICPMS Major and Trace Element Analyses

Rock and core samples had weathered surfaces removed, and were crushed and milled in preparation for X-Ray Fluorescence (XRF) Spectrometry disc production. A tungsten carbide mill was used in production of the crushed samples, so extreme caution must be taken when using W and Co data. Between 100 ppm and 220 ppm Co, and 950 ppm and 1,770 ppm W could have contaminated the samples over a 30–180 second grinding period (Cruickshank and Pyke, 1993). Consequently W and Co analyses have not been interpreted in this report. Fused glass discs and pressed powders were made from the crushed samples to run major and trace element analyses respectively. Major elements analysed using XRF are: Al_2O_3, CaO, Fe_2O_3 (total iron as Fe^{3+}), K_2O, MgO, MnO, Na_2O, P_2O_5, SiO_2, SO_3, TiO_2. Trace elements analysed using XRF are: As, Ba, Bi, Ce, Co, Cr, Cs, Cu, F, Ga, La, Mo, Nb, Nd, Ni, Pb, Rb, Sc, Sr, Th, U, V, W, Y, Zn, and Zr.

X-ray Fluorescence Spectrometry at Geoscience Australia is carried out using a Philips PW2404 4kW sequential wavelength dispersive spectrometer fitted with a Rhodium X-ray tube. It is used to measure the major elements present in samples, and a range of the more abundant trace elements to complement those analysed by the Inductively Coupled Plasma Mass Spectrometer (ICPMS). The XRF is calibrated using a range of Certified Reference Materials. The method used is a variation of Norrish and Hutton (1969). The detection limits for XRF analyses are shown in Table 6. Ga and Bi detection limits are unavailable.

Solution ICPMS analyses are carried out using an Agilent Technologies 7500ce ICPMS. Fused glass discs made for XRF major analyses are digested in acid, and run as solution samples through the ICPMS. Forty five trace elements are commonly analysed for, and concentrations in the ppb range are routinely obtained. Trace elements analysed, and expected detection limits can be seen in Table 6.

Table 6: Detection limits for Geoscience Australia laboratory instruments used in this study.

XRF major element detection limits (wt%):

SiO_2	TiO_2	Al_2O_3	Fe_2O_3	MnO	MgO	CaO	Na_2O	K_2O	P_2O_5	SO_3	LOI
0.006	0.002	0.001	0.002	0.001	0.004	0.002	0.004	0.002	0.001	0.001	0.001

XRF trace element detection limits (ppm):

As	Ba	Ce	Co	Cr	Cs	Cu	F	La	Mo	Nb	Nd
2	8	10	2	2	8	1	50	6	1	1	10
Ni	Pb	Rb	Sc	Sr	Th	U	V	W	Y	Zn	Zr
1	2	1	2	1	2	2	2	3	1	1	1

ICPMS trace element detection limits (ppm)

Ag	As	Ba	Be	Bi	Cd	Ce	Co	Cr	Cs	Cu	Dy
0.6	0.5	0.6	0.3	0.2	.02	0.03	0.2	1.5	0.03	0.8	0.05
Er	Eu	Ga	Gd	Ge	Hf	Ho	La	Lu	Mo	Nb	Nd
0.02	0.02	0.2	0.01	0.2	0.01	0.01	0.05	0.01	0.3	0.2	0.2
Ni	Pb	Pr	Rb	Sb	Sc	Sm	Sn	Sr	Ta	Tb	Th
2.5	0.15	0.02	0.15	0.8	0.5	0.4	0.1	0.5	0.05	0.01	0.05
Tl	Tm	U	V	W	Y	Yb	Zn	Zr			
0.1	0.02	0.01	0.5	0.1	0.1	0.03	0.6	0.2			

After analysis, XRF major element data was recalculated to provide oxide values as weight percent and elemental values in ppm. Fe_2O_3 data were corrected for FeO content after iron titration data became available. Raw Fe_2O_3T (Total), corrected Fe_2O_3, FeO, Fe^{3+} and Fe^{2+} have all been included in the final products to enable plotting of the multitude of diagrams available for iron species.

The unexpectedly very high Ba concentrations in some samples (up to 19,762 ppm) exceed the standard trace element calibration capabilities. Ideally Ba would be re-run as BaO on the major elements discs to get a complimentary Ba indication and rule out any potential detection saturation issues. As this was not done, Ba values should be treated with some caution.

XRF major element totals have not been normalised to 100%, thus wt% oxide and ppm values reflect the uncorrected Loss on Ignition (LOI) analyses. LOI values are predominantly minimal (<2% LOI= 59% of samples, <5% LOI = 90% of samples). Ten percent of samples show LOI >5%; these are primarily siltier lithologies or pebble conglomerates with altered matrices, and more weathered field and drillhole samples (high clay content). Four of these samples are from DH 139594 (PSC4/SASC2) and DH 9607 (ERD8), and are yet to be confirmed as Pandurra Formation. They are recorded as Whyalla Sandstone and undifferentiated Umberatana Group sediments in SARIG, and so have been disregarded in the 3D geochemistry interpolation.

Fe Titration

As iron valence cannot be measured accurately using the XRF, iron titration is used to determine the amount of FeO in samples. This can then be used to correct the Fe_2O_3T analysis from the XRF. Crushed samples are used in the ferrous iron determination process (as modified from Shapiro and Brannock, 1962). The samples are digested in HF, heated, and have indicator reagents added. The resultant solution is titrated using a potentiometric titration indicator. Geoscience Australia uses a Metrohm 716 DMS Titrino, with a Pt wire electrode. The detection limit for FeO titrimetry is 0.1 wt%.

Carbonate Identification

Upon receipt of the XRF geochemistry results, some anomalously high LOI results were noted. These samples typically have co-located Ca and Mg anomalies suggesting possible presence of carbonate. Six samples with similar SiO_2 values, and a range of LOIs were submitted for carbonate 'bomb' and XRD carbonate analysis. For the carbonate bomb test crushed sample and orthophosphoric acid are reacted in a closed cylinder with a pressure gauge attached. The degree of pressure change records the amount of CO_2 released, which can then be converted into weight percent carbonate. For XRD analysis crushed samples are loaded into a sample cup and analysed using the Seimens D500 XRD and Siroquant software. The resultant spectra are then interpreted to determine the minerals present in the sample. The use of both these techniques together identifies if the high LOI results are due to carbonate-derived CO_2, and the species of carbonate minerals.

HyLogger

HyLogger data for 65 drillholes within the Cariewerloo Basin were acquired from DMITRE. These 65 drillholes are not necessarily the same as those that have been physically inspected for this study, and as such the degree of drillhole control for interpreted HyLogger results in a given area may differ from the degree of drillhole control on a sedimentological or geochemical result interpreted in the same area. These HyLogger data allow the geochemical identification of subtle mineralogical gradients. The HyLogger data

used in this study are phengite-muscovite mica system specific, and are used in the assessment of fluid flow pathways, alteration, fluid temperature, and proximity to mineralised ore-bodies. The full methodology for using HyLogger data to interpret fluid and temperature conditions can be found in van der Wielen and Korsch (2005). The data consist of .csv files with both textual mineral identifications from spectral analyses in The Spectral Geologist (TSG) software, and numeric values for mica wavelength, abundance, and crystallinity. These data were imported into GOCAD as point files then interpolated to populate the voxet.

3D Methodology

Data preparation

This section provides a brief summary of the processes used to generate the 3D datasets in this report. Methodologies used to construct 3D objects are highly varied and strongly dependent on the input datasets and the intended purpose of the resultant objects. As this report is very specifically intended as an integrated assessment of the Pandurra Formation and the Cariewerloo Basin, the methodology is likewise specific. All data are projected in 3D space relative to the interpolated 1 second DEM surface (Gallant, 2011).

Simplification of pre-existing geology data for modelling

Geology polygons from the geol100mga53 (SARIG, 2009) GIS dataset were used in the production of the geology surfaces. These data are nominally 1:100,000 in scale, but is, on closer inspection a blend of both 1:100,000 and 1:250,000 geology data. Given the focus of this study is exclusively the Pandurra Formation, the geology polygons were simplified by time period to reduce the number of stratigraphic units from 296, to something more manageable. The challenge was leaving enough geological detail present to enable accurate rendering of the Pandurra Formation surfaces, but reducing the number of units present sufficiently to ensure the modelling could be achieved in the desired time frame. The number of stratigraphic units was ultimately reduced to ten.

The original stratigraphic dataset was resampled to give ten geological subdivisions: Cenozoic, Mesozoic, Paleozoic, Neoproterozoic, Pandurra Formation, Mesoproterozoic (all Mesoproterozoic units other than the Pandurra Formation), Gawler Range Volcanics (GRV), Hiltaba Suite, Paleoproterozoic, and Archean. The Cenozoic subdivision was ultimately omitted from modelling as the DEM surface acts in its place to provide the top surface of the model. Those units with age ranges that crossed over between two of the simplified subdivisions, those polygons listed as ‘miscellaneous’, and those with non-conforming stratigraphic codes were dealt with on a case-by-case basis, and slotted into whichever subdivision seemed to make the best geological sense. This included evaluation of how many polygons there were, the size of the polygons, and the surrounding polygons involved. A somewhat unexpected advantage arising from the simplification process was the great reduction in map sheet edge artefacts that were quite prevalent in the original dataset. Once the individual geological units to be combined into each new age subdivision were identified, the final simplification was achieved using a series of scripted dissolves in ArcGIS. The simplified geology polygons were then imported into GOCAD and draped on the DEM ready for surface generation. Figure 6 below shows the complexity of the original State MGA 1:100,000 dataset as compared with the simplified geology polygons used in this study.

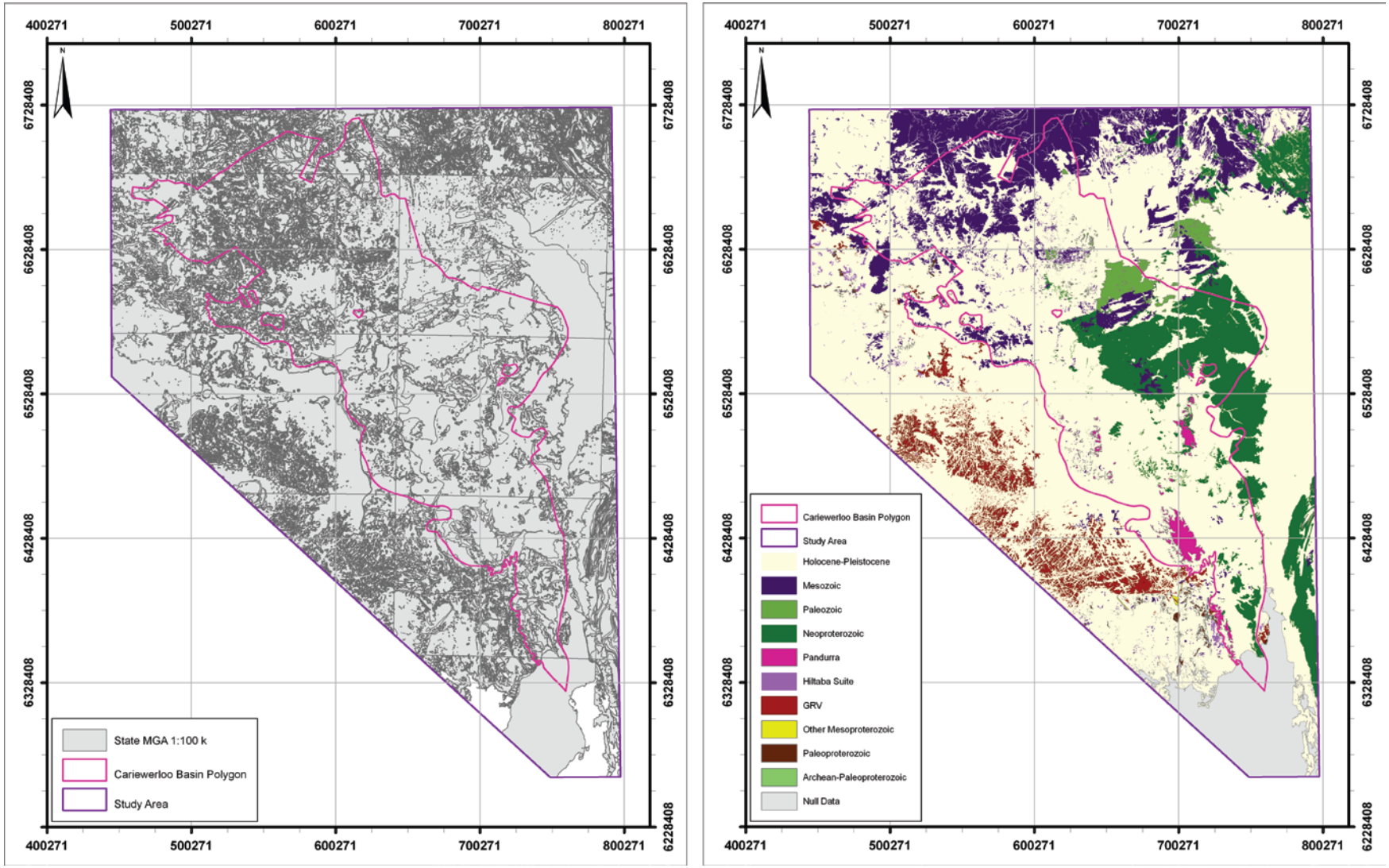

Figure 6: *Line work of State MGA 1:100,000 geology (SARIG, 2009) (left) and simplified geology polygons generated for this study (right) for comparison. Cariewerloo Basin Polygon (SARIG, 2011) shown as pink curve for reference.*

In addition to the geology polygons, the Cariewerloo Basin Polygon (SARIG, 2011) was also used to constrain the surfaces. Unfortunately the basin polygon does not encompass key field localities at Red Rock and Mt Laura, and a new field locality at Wirraminna Station, which are all on the western edge of the basin. The drillholes SLT101, BLD2, Bumbarlow1, ERD9, ERD8, and WokurnaDDH6 (DH 25360, 20831, 104376, 9608, 9607, and 29739 respectively) that are being considered for inclusion in the Pandurra Formation also fall outside the current Cariewerloo Basin polygon. A slightly modified Cariewerloo Basin polygon was used to define the boundaries of the voxet, and, despite the fact these data points fall outside the main voxet area, these data have still been used to inform the grain size interpolation process.

Drillhole data

Drillhole data to be used for surface generation were selected by location from the ArcGIS database DH_STRAT (SARIG, 2011); using the study boundary and a 'within' spatial query. Of the selected 6,366 drillholes, those with no meaningful stratigraphic information, and those <5 m long were discarded. Those drillholes identified as having more than ten stratigraphic units down hole were corrected manually using SARIG data to add in units lost in the process of database loading (the DMITRE database appears to automatically truncate entries longer than ten stratigraphic units). Drillholes with inadequate location, dip, azimuth, and measured depth (MD) information were also corrected manually using SARIG data where possible, or deleted if not. Twelve drillholes newer than the DH_STRAT dataset were added manually using data from SARIG. These drillholes were AMD1, SH7, and the ten ARIES drillholes. Drillhole collar elevations were extracted from the GOCAD DEM surface to ensure an internally accurate dataset. These Z values can be found alongside the final drillhole data in the digital appendices. Drillholes directly on the boundary of the study area, and those far outside the main study area (e.g. WokurnaDDH6, DH 29739) beyond the GOCAD DEM boundary had collar elevations extracted from the original 1s DEM (Gallant, 2011) in ArcGIS. The locations of drillholes used for surface building are shown below in Figure 7.

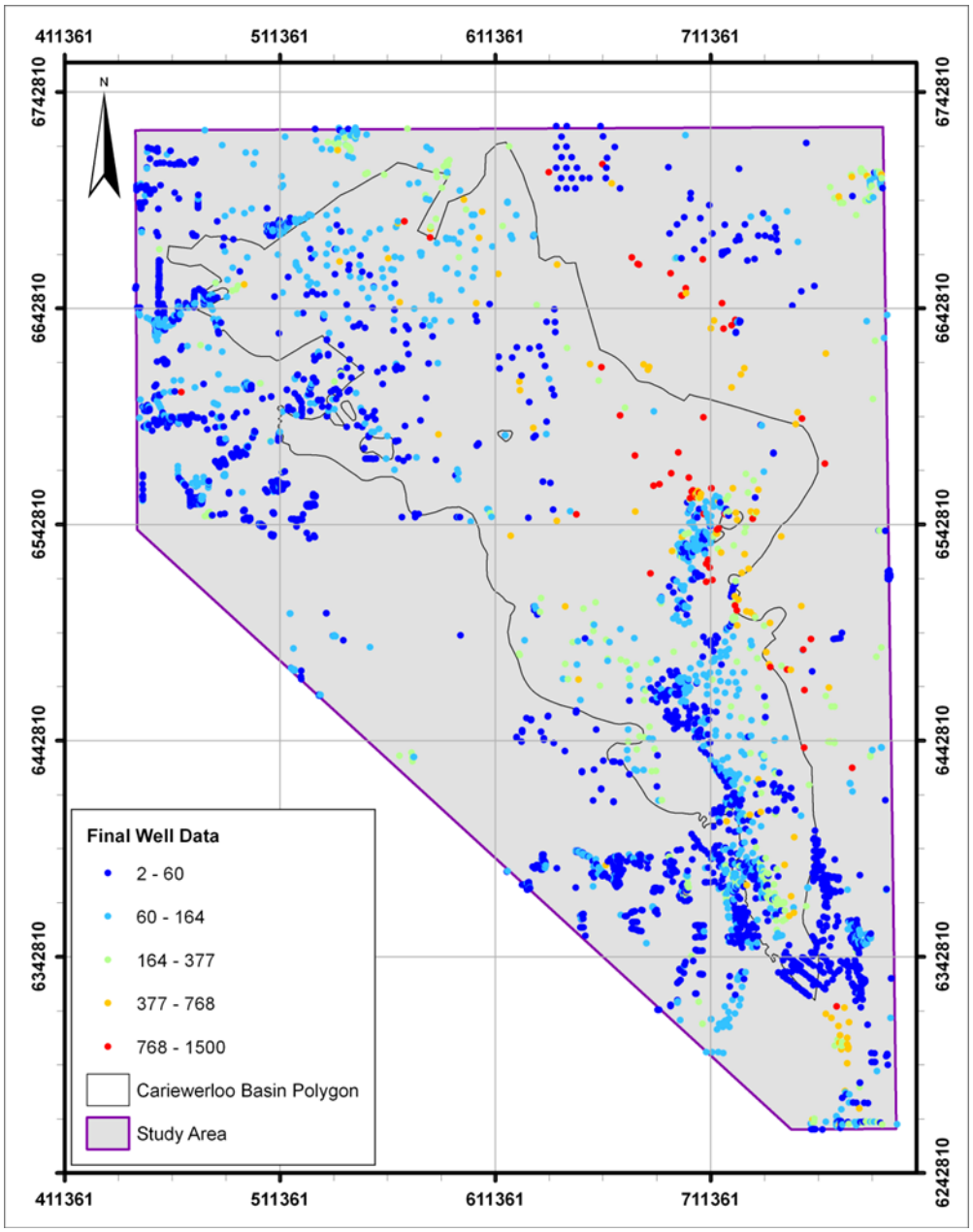

Figure 7: *Locations of drillholes used for surface building. Drillholes are coloured according to maximum drilled depth (in metres). The Cariewerloo Basin Polygon (SARIG, 2011) and Study Area polygon are included for reference.*

Five thousand nine hundred and thirty two drillholes passed the initial QA/QC process to be used in the generation of the geological surfaces. The stratigraphic information for these drillholes was simplified to represent the same geological subdivision as the geology polygons described previously. This process reduced the number of units from approximately 276 to ten. Stratigraphic codes were used to facilitate the simplification process. The stratigraphic codes were converted into numeric codes and replaced by their new overarching simplified code. Duplicate code entries for each drillhole were then identified in excel, which were then simplified. In the process of this simplification, intrusive units such as the Gairdner Dykes were removed from the drillhole stratigraphy. These relatively small-scale and discontinuous lithologies are beyond the scope of the modelling used in this report. The final drillhole data used in surface production is included in the digital appendices as Dillhole_Markers_As_Bottoms.gp, and Drillhole_Markers_As_Tops.gp. Grain size curves from drillholes physically inspected for this study were added as 'well logs' in GOCAD. These drillholes are included in the digital appendices as a separate

dataset for ease of use (as individual .wl files, and as a group file 'Logged_wells.gp'). In the process of populating the voxet with grain size data, the grain size well logs were resampled at 1.0 m and converted to points in order to facilitate timely data processing without sacrificing too much detail. The original resolution grain size data has been included digitally for viewing and to meet future possible processing requirements. Field grain size transects and point data were loaded into GOCAD and Z values were adjusted by 10 m to force the points beneath the DEM (and hence within the voxet) to act as further constraints in the grain size interpolation process.

Faults

Faults used in the 3D modelling process are modified from the dataset Faults_tectonic_interp_lines.pl from the Cariewerloo Basin Unconformity-related Uranium Project Data Release (Wilson et al., 2011). The other fault datasets from this data release have been included in the digital appendices of GOCAD files for comparison. Of note are the Fault_interpreted_worms.pl faults which have been interpreted from magnetics data using multi-scale edge techniques. Some of these faults appear to have some geochemical significance, coinciding with the 'geochemical trend lines' identified during this study. In the absence of other constraints, all faults used in the generation of 3D datasets for this study have been considered vertical.

Gravity Magnetics and Radiometrics

Combined Bouguer gravity data, Reduced to Pole (RTP) magnetic data, and radiometric data (Bacchin, et al., 2008; Milligan, et al., 2010, and Minty et al., 2010 respectively) have been used to assist in general interpretation of the Pandurra Formation, the Cariewerloo Basin and associated faults. They were incorporated into the 3D model initially as point sets extracted from the original grid, then as triangulated mesh surfaces (with gravity values in $\mu m/s^2$ used for Z, and magnetic values in nT used for Z).

Geochemistry

Geochemical data were loaded into GOCAD as two point datasets. One contains only the XRF data used to interpolate the voxet properties. The other includes the ICPMS results that were generated this study, but not used for interpolation purposes. In the XRF dataset the property "Pandurra' codes the samples for current Pandurra Formation status to enable identification of samples from the additional Pandurra Formation drillhole and field localities. These samples were not used in the interpolation of the geochemistry voxet properties.

Surface Generation

DEM Surface

A DEM surface was constructed from a resampled (50 m) grid of the national 1 second DEM (~29 m grid, Gallant et al., 2011) using the optimisation routine shown below in Figure 8 (from van der Wielen et al., in prep). Optimisation varies the size of the mesh triangles using small triangles in hilly terrain, and large triangles in flatter regions against predefined tolerances. This process significantly reduces the file size of the final triangulated mesh, while honouring the original DEM grid.

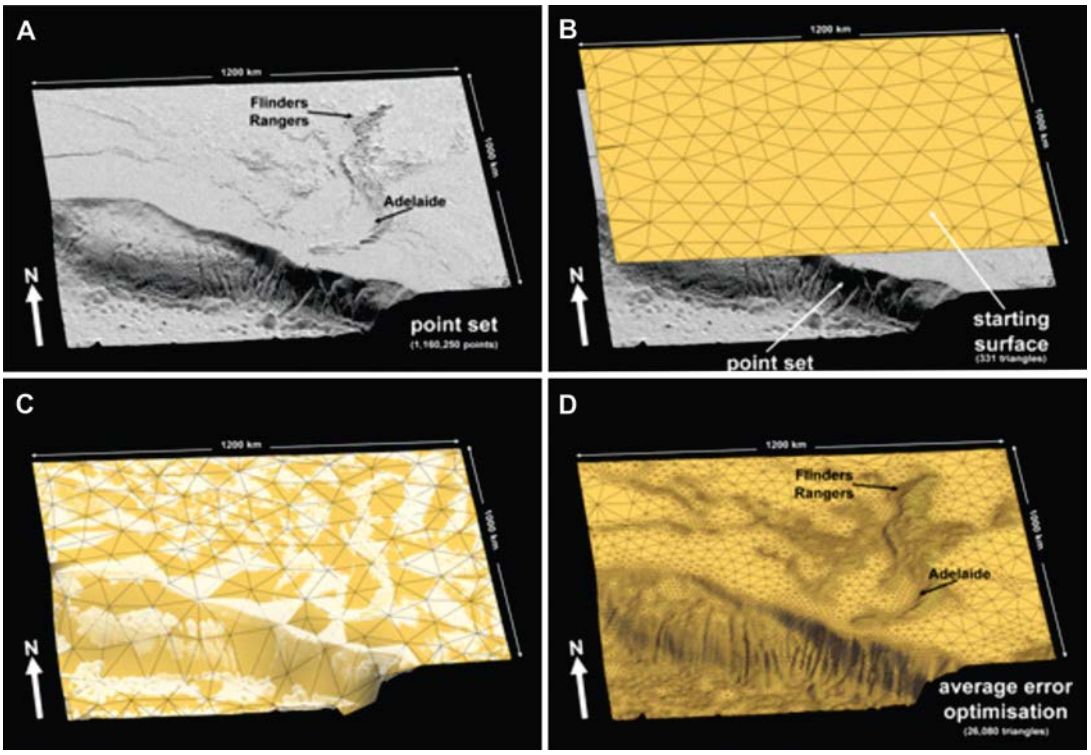

Figure 8: *Images showing the optimisation process used to create the DEM surface. A point set is extracted from the DEM grid using ArcGIS and imported into GOCAD (a); an initial surface is created with a coarse triangulated mesh (b); the initial surface is then moulded to the DEM point set (c); and average error surface optimisation run (d). Progressive iterations of steps (c) and (d) are used to improve the surface. Eleven iterations were used in the generation of the final DEM used in this report. Figure from van der Wielen et al., (in prep).*

Geological Surfaces

The ten simplified geological subdivisions were built as surfaces from the top down (youngest first). The draped geology polygons and simplified drillhole geology were the underpinning data in the production of the geological surfaces. It is common practice to use the geology polygons and drillhole data to manually interpret the geology, and generate a boundary curve that forms the edge of the geological surfaces. The manually interpreted boundary curves thus control the lateral extent of the geological surface. For this study a new approach was taken where no time-consuming boundary curve generation was undertaken. Instead the study area polygon was used to form the initial surface boundaries.

Four sets of constraints were used in the generation of the surfaces, two of these are very ‘traditional’ and two were being used for the first time in this study. The well markers and geological polygons datasets were modified and converted into point sets to form the traditional two constraints datasets to which the geological surfaces are fitted. The well marker dataset was modified to force well markers that fall within their own geological polygon above the DEM. This accounts for the fact that these markers do not actually represent the true ‘top’ of the geological unit – rather the eroded surface. For the first ‘non-traditional’ constraints dataset, a randomised point set filling the inside of each of the simplified geology polygons was generated in ArcGIS and imported into GOCAD. These points form the ‘internal_points’ datasets. The points were initially draped on the DEM to reflect the present day topography. Z values were then adjusted upwards by 100–150 m so the points fell well above the DEM (i.e. DEMz+150 m = ‘internal_points’z). These points provide an ‘inside/outside’ control during interpolation, forcing the optimisation process to honour the geology polygons at the ground surface. For the second ‘non-traditional’ constraints dataset, the ‘internal points’ datasets were used in a second process to make the ‘older units points’ datasets. These are different for every surface as only the ‘internal geology’ point sets for geological units older than the surface need to be used as constraints on the surface currently being produced. Together these four sets of

constraints function to push the surface above the DEM where required, cut through the DEM where the geology polygons are present, and honour the well markers. Once the constraints for each geological surface were compiled surface construction could begin.

The initial surfaces were created using the 'create surface from closed curve' function. The surfaces were then optimised to fit the constraints using the process outlined for the DEM surface. Surfaces were then cut progressively using the surfaces younger than the surface in question. For example: the Mesozoic surface was cut by the DEM, while the Paleozoic surface was cut by the DEM and then by the Mesozoic surface. After each surface intersection, the unwanted parts of the surface being cut were deleted. It is this surface intersection process that largely defined the lateral geological extent of surfaces in this study. Minor manual constraints were then imposed on the Pandurra Formation surfaces particularly at the margins of the basin, where well constraints are minimal. As a final step, surfaces were cut by previously generated fault surfaces (line work from PIRSA Faults_tectonic_interp_lines.pl, Wilson et al., 2011). Approximate relative displacement across faults was determined by analysing surface geology and drillhole data.

Only the Pandurra Formation geological surfaces were used to build the voxet. This is because the modelling of grain size and geochemistry is focused on the sedimentary rocks within the Cariewerloo Basin. To facilitate the voxet building process, bounding surfaces were generated to contain the basin. These are simple synthetic surfaces generated from the study area curve and the Cariewerloo Basin Modified Polygon. Together with the fault surfaces, these synthetic surfaces completely enclose the Pandurra Formation, and delineate the final 3D voxet volume. The surfaces to be used in later voxet generation were checked to ensure that they were watertight with no holes or overlaps between the surfaces.

Voxet Generation

Voxets are a proprietary GOCAD block modelling approach that enables both 3D visualisation and spatial queries. The Pandurra Formation voxet created in this study covers the study area with a cell size of 1,000 m x 1,000 m x 10 m and contains 32,568,981 cells. The cell size has been chosen to try to capture the highly variable resolution of the data to be contained within the voxet, as well as be computationally feasible in a reasonable space of time. The following procedure was used in voxet construction:

- A blank new voxet was created using 'create voxet from step vectors' function in GOCAD (Mallet, 1992b). This function produces a blank voxet containing no properties or regions – the cage the final voxet will ultimately be built within.
- The Upper and Basal Pandurra Formation surfaces, synthetic bounding surfaces, fault surfaces, and the DEM surface were all added to the empty voxet. Using the build function, regions were created from the surfaces. This generates many small regions within the boundaries of the surfaces.
- Two voxet properties ('id' and 'rock_unit') were created. The 'id' property was used to store the numeric suffix from the region name (i.e. 123 for Region_00123). This was done so that it was possible, if necessary, to regenerate regions from the 'id' property. The 'rock_unit' property was created to attribute the voxet with geological units.
- After careful inspection of the resultant small regions, each small region was assigned to the desired final geological region. The four final regions used for this study were: 'Air' (above DEM), 'Cover' (area immediately above Pandurra within the Cariewerloo Basin Polygon), 'Pandurra', and 'Basement' (all rock outside the Cariewerloo Basin). To assign each small region to its final geological region, the compute function (property script editor) in GOCAD was used to attribute the id and rock_unit using the following script: if (region == Region_000n) {id = n && rock_unit = x;} where n is the region's numeric suffix and x is the corresponding geological unit. This process combined the many small regions generated initially, into the final four regions.
- The final regions were then attributed with the desired colour and the completed voxet saved.

This basic voxet can then be populated in 3D with any property and can then be spatially queried. To this end, the grain size and geochemistry data generated during this study, and the DMITRE HyLogger data (SARIG, 2012) were gridded in 3D using GOCAD's Discrete Smooth Interpolator (DSI) algorithm (Mallet, 1992a). In addition, several calculations including distance to faults, distance to DEM, and distance to unconformity were calculated and have been included as properties in the final voxets. To enable running the GOCAD files on a standard high-end machine a geochemistry and grain size voxet, and separate geophysical voxets have been created. These voxets form the basis of the 3D sedimentological and geochemical assessment of the Pandurra Formation.

Comments on 3D Methodology and Limitations

In general the methodology used to generate the data released within this report is regarded as reasonable. The major limitations identified are listed briefly below, and in more detail in the paragraphs following. Some comparisons are drawn between the Cariewerloo Basin data release (Wilson et al., 2011) and this 3D release to evaluate the methodology used this study.

- The uneven distribution of drillhole data across the study area resulted in difficulties choosing the final voxet resolution. This has subsequently resulted in the generation of artefacts in areas with limited data. This directly relates to the Discrete Smoothed Interpolation (DSI) issue identified below.
- Simplifying geology by time period in the surface-rendering process appears to have done a reasonable job of rendering the Pandurra Formation surfaces, but ideally would be modelled at full geological resolution (i.e. every geological unit modelled as a separate surface) in order to better resolve the orientation and continuity of faults within the Cariewerloo Basin.
- The 1 m averaging of high-resolution HyLogger and grain size data allows major trends to be identified. However, removing the need to degrade data resolution would be ideal.
- Using a limited selection of vertical faults, and forcing these to penetrate the full thickness of the voxet, with largely unknown dip and displacement data is unrealistic.
- Interpolating grain size with no numeric limits, and subsequently classifying this data has produced over representation of grain size <0.04 mm, as true alteration and shale data are being smoothed into the 0.04 mm grain size classification. Some limitation on this smoothing process is needed in order to remove the confusion between true alteration zones as seen around Emmie Bluff and alteration zone artefacts generated during the interpolation process.
- Other limitations associated with DSI interpolation of properties through final voxet and subsequent artefact generation, such as dipole anomalies.

Given the emphasis on the Pandurra Formation in this study, minor discrepancies in the rendering of the younger geological surfaces have been left in place where they have little impact on the final shape of the Pandurra Formation surfaces. These discrepancies are located in areas where the geological units are very thin and/or laterally discontinuous. This includes the southern tip of the Cariewerloo Basin where units are very thin, and in the middle of the far northern study area where the geological units are highly discontinuous. The surfaces of geological units older than the Pandurra Formation (GRV, Hiltaba Suite, Paleoproterozoic, and Archean) have been used collectively to inform the basal Pandurra Formation surface, and have been included in the data release, but it is strongly advised against using them for other purposes. Few constraints exist to determine the shape of these basement surfaces, and as they are not the focus of this study, they have not been rigorously corrected.

In the process of generating the surface constraints, the draped geology polygons were converted into points. These points were left sitting at the DEM elevation for the surface interpolation process. If this method is to be used again, dropping these points just below the DEM is recommended as having these points exactly coincident with the DEM surface made the final surface cutting/part deletion process difficult. It also generated a few bad triangle artefacts in the final surfaces.

The modified surface generation process worked very well in areas where there are reasonably dense constraints to control the lateral extent of the surfaces. In places with very few constraints this method results in surfaces that extend laterally for geologically unrealistic distances. This is why boundary curves are usually enforced on the surfaces at the start of the traditional surface building method. The method used in this study allows the available data to be modelled with minimal bias that a geologist's interpretation of

3D geological extent can impart during the boundary curve generation process. It does however need to be used with caution. Some combination of first-pass surface generation using the method developed during this study, in conjunction with geologist-imparted interpretation to add extra constraints where necessary (as was ultimately used this study) may provide a 'best of both worlds' solution. An example of where this combined approach would work well occurred during the generation of the Pandurra Formation surfaces. The lack of any drillhole constraints to the east of the Cariewerloo Basin left the surfaces extending far to the east, most likely beyond the true extent of the Pandurra Formation. The addition of a few extra constraints after the initial surface generation removed this artefact leaving a more realistic looking surface, while retaining the time saving and bias removing benefits of this method.

As briefly mentioned earlier, the Cariewerloo Basin Modified polygon was used to provide the lateral extents of the Pandurra Formation, to simplify voxet production and provide constraints where there were none. This polygon does not enclose all of the Pandurra Formation outcrops or well markers. However, in the process of populating the voxet with grain size and geochemical data those Pandurra Formation occurrences outside the Cariewerloo Basin (and the associated data) have been considered in the interpolation process. So while these Pandurra Formation occurrences are outside the voxet, their data have not been ignored. Redrawing the Cariewerloo Basin polygon to include the Pandurra Formation occurrences currently outside the basin (from SARIG) has been addressed briefly here to include some of the 'extra-basinal' known Pandurra Formation occurrences (see Figure 9 below), but needs to be considered more comprehensively in the future. Communication with DMITRE indicate that an updated Cariewerloo Basin Polygon has been completed since this report was commenced, but that the SARIG update is also reliant on the updating of the SA solid geology and so could take some time to implement in full (Tania Wilson, pers. comm., 2012).

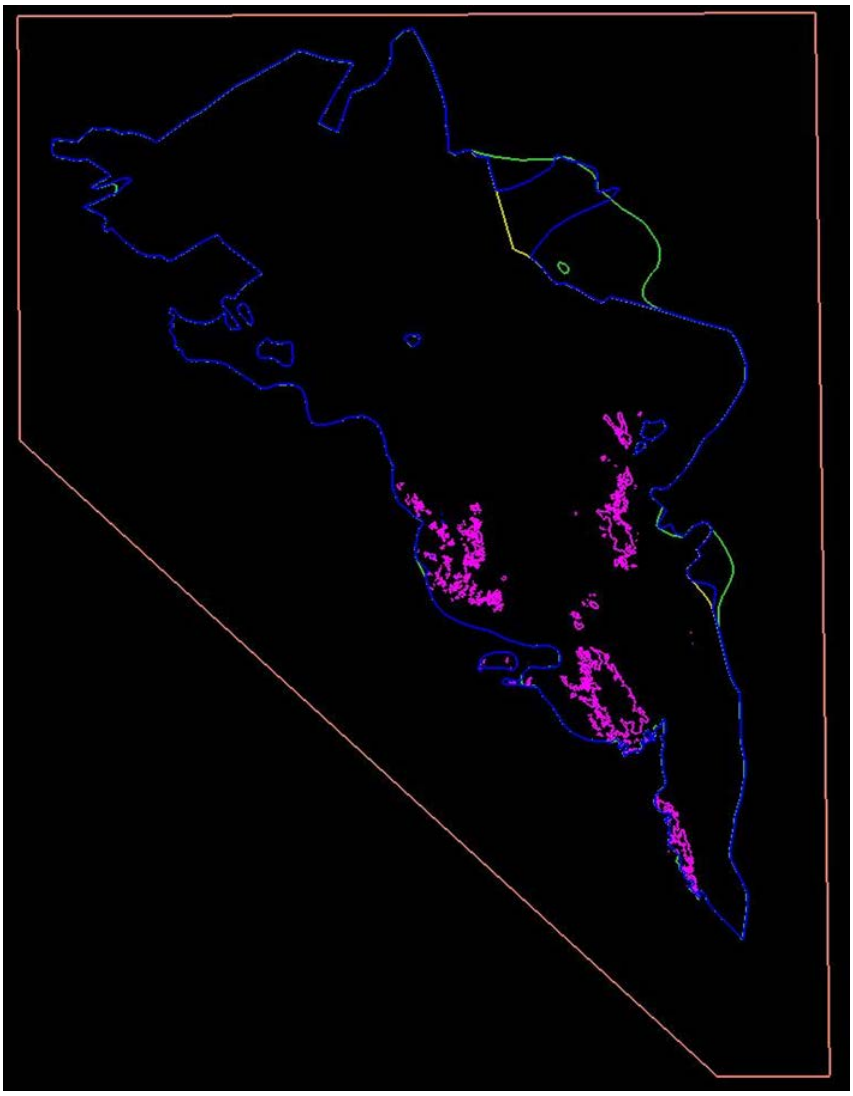

Figure 9: *Modified Cariewerloo Basin Polygon as used for voxet generation (blue) with the original Cariewerloo Basin Polygon (yellow, SARIG, 2011) and the suggested Modified Pandurra Boundary Curve (green). Areas that appear speckled occur where polygons overlap. The study area curve (peach) and Pandurra Geology Polygon (pink) are also shown for reference.*

Surfaces

A comparison with existing interpretations has been completed comparing the Pandurra Formation surfaces as built for the Cariewerloo Basin data release (Wilson et al., 2011) and those built in this study. This comparison is used to check for surface rendering issues, particularly given the new methodology used for this study.

The DMITRE study (Wilson et al., 2011) used Pandurra Formation penetration and intersection data updated from Cowley (1991), drill-hole data from SARIG, points within the Pandurra Formation surface geology polygons, and control points derived from Airborne Electromagnetic data (AEM), to render the Upper and Basal Pandurra Formation surfaces. Collectively there were 6,616 control points used to generate the initial surfaces.

The current study relied on modelling the greater geological context of the Pandurra Formation, and as such modelled the over- and under-lying geological surfaces to better control Pandurra Formation surfaces in areas where limited drillhole intersections were available. This study used data from 5,931 drillholes and in

excess of 13,000 well markers (drillhole intersections) in addition to the known Pandurra Formation penetrating drillholes (398 drillholes) and intersecting drillholes (67 drillholes) data. Collectively these datasets provided many thousand control points for each geological subdivision to enable the rendering of the Upper and Basal Pandurra Formation surfaces. In addition, all the geological surfaces were slightly modified where necessary prior to final Pandurra Formation surface rendering in order to produce geologically realistic interpretations and thus adding another layer of geological realism. However, it is noted the confidence assignation process used during the DMITRE surface-rendering in order to differentiate between high confidence Pandurra Formation well marker locations, and lower confidence well marker locations was not used in this study. Certainty in well marker location was only assessed and adjusted for drillholes that were physically logged this study. Outside this group of 67 drillholes the SARIG well markers were generally taken as accurate, unless obvious stratigraphic or typographic errors were recognised during the drillhole data simplification process, and subsequently cross-checked against and corrected using company log data.

The most obvious difference between the Upper Pandurra Formation surface constructed in the DMITRE study and in this study is the modified Cariewerloo Basin extent used in this study to include some of the interpreted Pandurra Formation occurrences on the east side of the basin, and the elevated surface around SSR1001 (DH 16638) in the centre of the basin. Relatively minor exaggerated surface elevation of the DMITRE surface relative to the Upper Pandurra surface from this study is also observed in areas of extreme topography, and along the basin margins. Around the margins of the basin the Upper Pandurra Formation surface of this study is better constrained than the DMITRE surface. The DMITRE surface also significantly penetrates the DEM surface, largely, but not exclusively within the Pandurra Formation surface geology polygons (note: apparently this artefact has since been corrected in the second data release http://www.pir.sa.gov.au/minerals/geological_survey_of_sa/geology/3d_geological_models/cariewerloo_basin_geological_model, Tania Wilson, pers. comm., 2013). Presumably this is because this surface was not made as part of a full voxet and so was not clipped by the DEM and subsequent geological surfaces, as the surfaces in this study were. Assuming this surface processing difference accounts for much of the DEM penetration, areas in the western north of the basin are still over-elevated penetrating the DEM in areas of no surficial outcrop. Where outcrop is mapped, the DMITRE surface does a good job of matching the surface geology polygons, with the western extreme of the Cariewerloo Station outcrop, and the outcrop around Mahanewo Station being the least well resolved. The Upper Pandurra Formation surface generated during the current study performs slightly better around Mahanewo Station, but likewise struggles to resolve the highly-detailed outcrop patterns around Cariewerloo Station (see Figure 1 for station locations). In terms of unwanted DEM penetration, there are a few sub-kilometre patches in the western north of the basin where the Upper Pandurra Formation surface from this study penetrates the DEM. This is due to very slight over-interpolation during surface creation which has not been corrected for as these small artefacts had no material impact on the geological interpretation.

The Basal Pandurra Formation surfaces from this study and the DMITRE study (Wilson et al., 2011) are also quite similar, with fairly uniform <150 m difference in surface elevation, and the extreme eastern edges of the central and southern basin again proving the most different. The area around BDH3 (DH 25356), SLT107 (DH 25357), and SLT101 (DH 25360) is relatively under-exaggerated in the DMITRE surface, where the very steep drop off across the faulted eastern basin margin to the very deeply buried Pandurra Formation is not honoured. In the extreme south of the basin, the Basal Pandurra Formation DMITRE surface does not extend to the basin margin, and does not match the margins of the Upper Pandurra Formation DMITRE surface either. Otherwise, the basal surfaces are generally quite similar, with minor differences at topographic extremes where the DMITRE surface is often shallower, and less smoothed. Figure shows the calculated numeric differences between the Pandurra Formation surfaces from this study and the DMITRE study.

While addressing the DMITRE data release, a very brief assessment of the DMITRE Pandurra Formation Member surfaces will also be made. These surfaces were not used to inform any modelling or interpretation in this study, as major limitations were detected. The four individual Member Surfaces cross-cut both each other, and the Upper and Basal Pandurra Formation surfaces. The Member Surfaces have also been quite

strictly clipped using the Member 1– 4 point sets. While it is commendable to limit the surface extents to relatively well-constrained regions, for the Member Surfaces released, and particularly for Member 2 where the shale lithology is concentrated, many known shales occur outside the Member 2 surface extent as it stands, and so the Member surfaces appear to have been unnecessarily truncated. Wells with shales outside the Member 2 surface area include DP2, Playford 1, LY1, RCDD04TI008, and possibly WY12 where a six metre of interval of lost core is likely to have been shale (DH 14058, 16699, 13909, 209917 and 14816 respectively). Due to these kinds of limitations, and the relative lack of assigned Member data, no attempt has been made to model the four Member Surfaces in this study. Instead isosurfaces of Pandurra Formation interpolated grain size have been created. These surfaces collectively enclose the 3D extent of particular grain sizes from shale (0.063 mm) to the coarsest conglomerates (64 mm +). It is hoped these isosurfaces and the grain size voxet will be more informative than the Member subdivision surfaces, as they relate more directly to fluid pathways and fault proximity and hence mineralisation potential. However, it is noted that these isosurfaces do not capture small scale variation in grain size and thus will give only regional-scale grainsize indications useful for regional scale fluid migration studies. The 0.063 mm, 0.05 mm, 1 mm, 4 mm and 16 mm isosurfaces are shown in plan view in Figure 18.

Geochemistry Voxet

The interpolation of the point geochemistry data from this study and the HyLogger mica well logs to represent 3D geochemistry in the voxet appears to have been successful as geologically reasonable geochemical anomalies were identified. The areas of lowest confidence are the central southern basin, and the north-west and central northern basin, where there is poor drillhole control. This is particularly evident in the interpolated data where a large area of longer wavelength mica is indicated in these two areas purely due to interpolation. Higher-resolution data in these areas are required to map the geochemistry in these areas before more accurate mineralisation potential mapping can be completed. Targeting the areas intersected by the four major geochemical trend lines identified this study would be a good starting point for exploration.

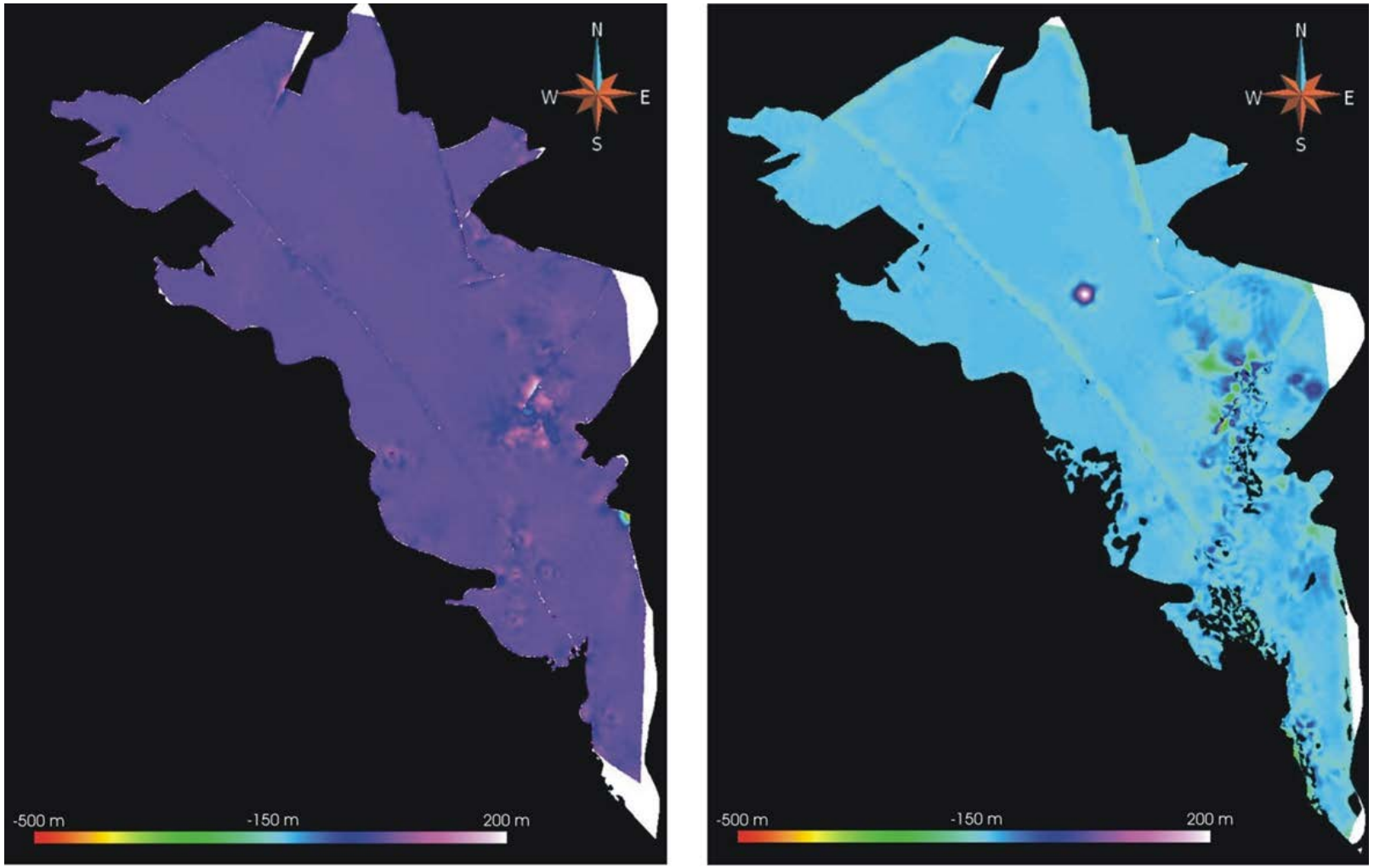

Figure 10: *Numeric comparison of the two Upper (left), and two Basal (right) Pandurra Formation surfaces from this study and the DMITRE Cariewerloo Basin data release (Wilson, et al., 2011) surfaces. White areas represent where the study area polygons are different, and so no overlap of the surfaces is detected. The colour ramp shows the numeric difference in surface elevation. The left image shows the numeric product of the Upper Pandurra Formation surface of this study minus the DMITRE equivalent. The right image shows the same calculation for the Basal Pandurra Formation surfaces.*

Examples of 3D Results

As modelled in GOCAD for this study, the Pandurra Formation occupies some 90,000 km^2. Example images of the geological surfaces, voxet, and 3D geochemistry results are included here.

Geological Surfaces and DEM

Ten geological surfaces and one DEM surface were created for this study, with the main aim being to determine the upper and lower surface of the Pandurra Formation. The ten geological surfaces being released are shown in Figure 11. The very thin nature of the younger units, the complex surface geology, and relative lack of data to constrain the deeper surfaces left a myriad of minor cross cutting surface errors after initial construction. Many of the errors have been manually resolved where data and/or geological context were available, and where they significantly impacted on the shape of the final Pandurra Formation surfaces. Areas of known remaining errors include the southern tip of the Cariewerloo Basin where units are very thin, and in the middle of the far northern extreme of the study area where the geological units are highly discontinuous.

The simplification of the geology by time periods was a useful approach for this study as it greatly reduced the 3D modelling time, and still produced better-constrained Pandurra Formation surfaces than would have been possible otherwise. A consequence arising from this approach is the relatively limited uses for the generalised geological surfaces. Not modelling the faulting of the Pandurra Formation in greater detail, however, is more concerning. Many more minor faults are known to cross-cut the Cariewerloo Basin than were modelled in this study. Only major faults, and the faults defining the basin margins, were modelled. The faults used in this study (Wilson et al., 2011) are shown cross-cutting the Basal and Upper Pandurra Formation surfaces in Figure 12. The purely vertical nature of the faults and the depth of fault penetration as implemented in the absence of other data are clearly visible, as is the minimal known displacement implemented for most of the faults.

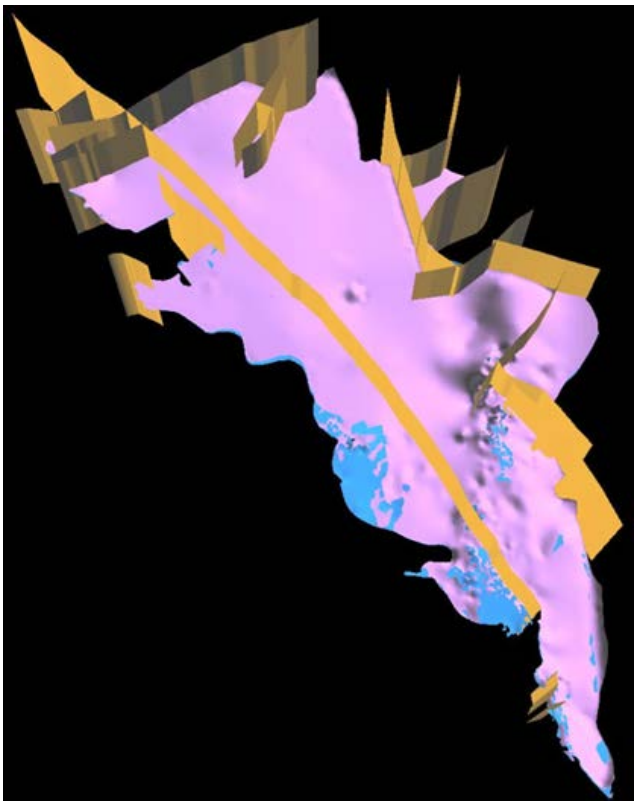

Figure 12: *Faults used in the voxet production as cross cutting the Basal Pandurra Formation Surface (blue) and the Upper Pandurra Formation Surface (pink).*

While the fault displacements appear to be relatively minor, using this voxet for investigating parameters like fault-controlled secondary porosity would not be realistic until the lack of faulting information has been resolved.

Pandurra Formation Surfaces

The Basal and Upper Pandurra Formation surfaces are shown in Figure 13, along with a Pandurra Formation thickness map. As indicated earlier, the Pandurra Formation surfaces were fitted to the grain size logs generated this study to reflect the interpreted length of Pandurra Formation drillhole sections, as compared to the SARIG well markers. A noticeable exception to this is the SAE3 (DH 165606) and SAE4 (DH 165607) grain size logs. These were not completed until after the rendering of the Pandurra Formation surfaces, and so these well logs penetrate the Basal Pandurra Formation surface quite significantly. This means the surfaces represent the thickness of the Pandurra Formation around these two drillholes more in accordance with the original SARIG well intersections in the area around Emmie Bluff.

As modelled, where the Pandurra Formation intersects the DEM, the blue Basal Pandurra Formation surface can be seen apparently intersecting the pink Upper Pandurra Formation surface in Figure 13. This reflects the fact that for modelling purposes, the Upper Pandurra Formation surface effectively is above ground level and so has been truncated by the DEM. The complex volume defined by the surfaces is best viewed in GOCAD voxet section, but the reduced sediment thickness in the west, and significant topography on both Pandurra Formation surfaces can be seen in Figure 13.

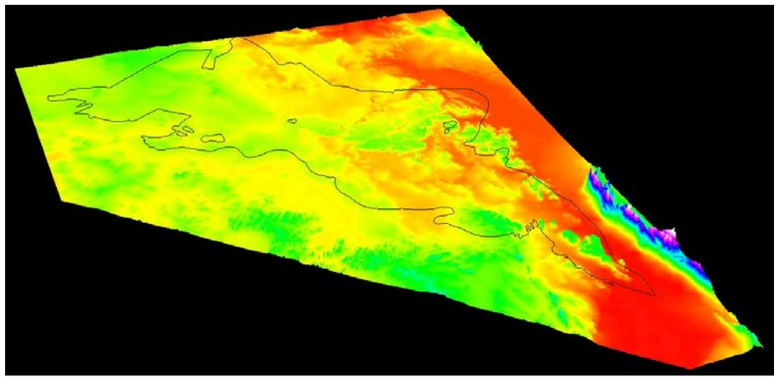

Figure 11: *Geological surfaces and DEM generated this study to enable Pandurra Formation surface construction. Surfaces are shown sequentially overlain from most basal to the DEM. The Cariewerloo Basin Polygon at 1000 m is shown in yellow (in black on the DEM), and the Study Area Polygon is shown in white at 0 m for reference. In ascending order the eleven surfaces are: Archean (brown), Paleoproterozoic (grey), Hiltaba Suite (yellow), Gawler Range Volcanics (GRV, white), basal and upper Pandurra Formation (pink and blue), other Mesoproterozoic (orange), Neoproterozoic (pale green), Paleozoic (dark green), Mesozoic (dark blue), and DEM (multicoloured, colour ramp by Z value). Inclined plan view, vertical exaggeration 20 x. The DEM surface acts as the effective Cenozoic surface, capping the top of the model and truncating all the other surfaces. The surfaces shown here are unfaulted.*

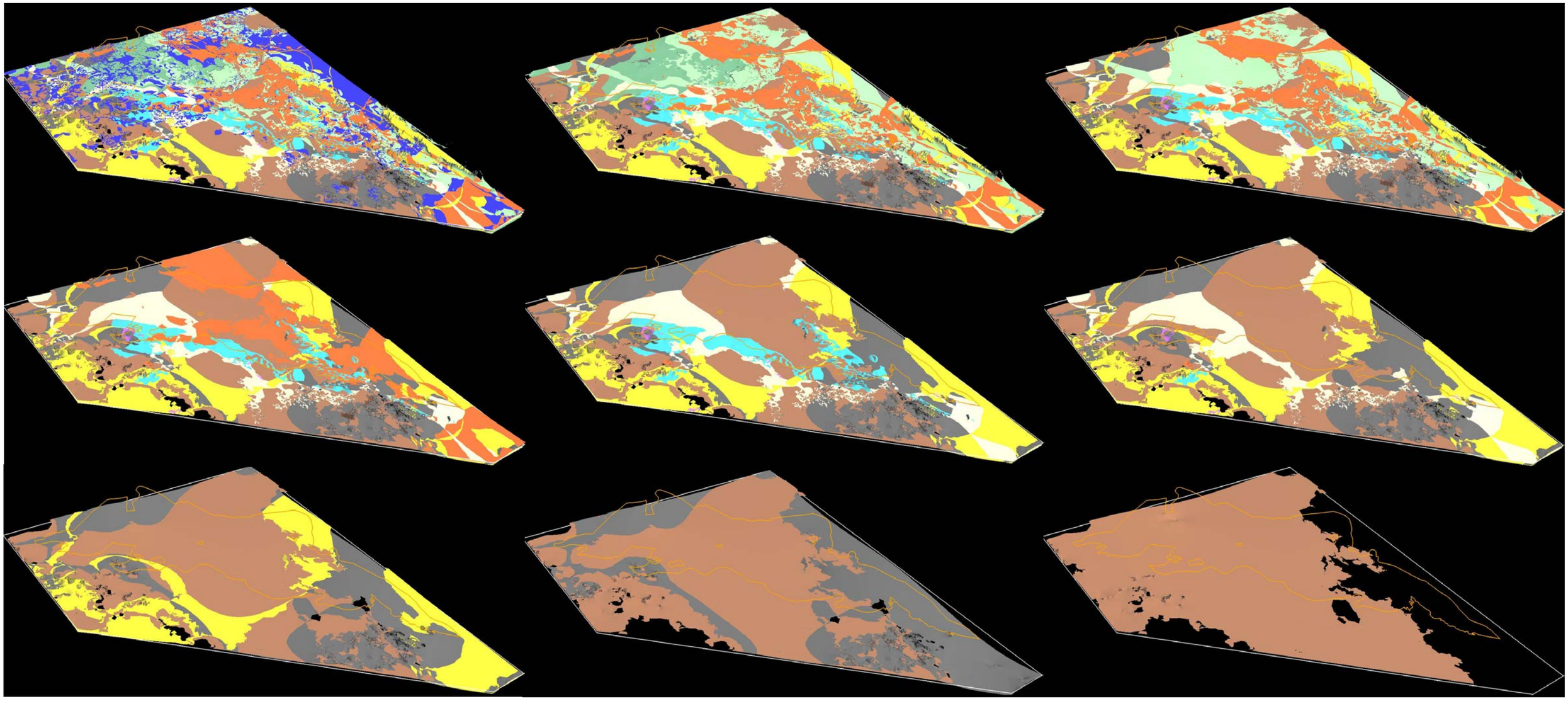

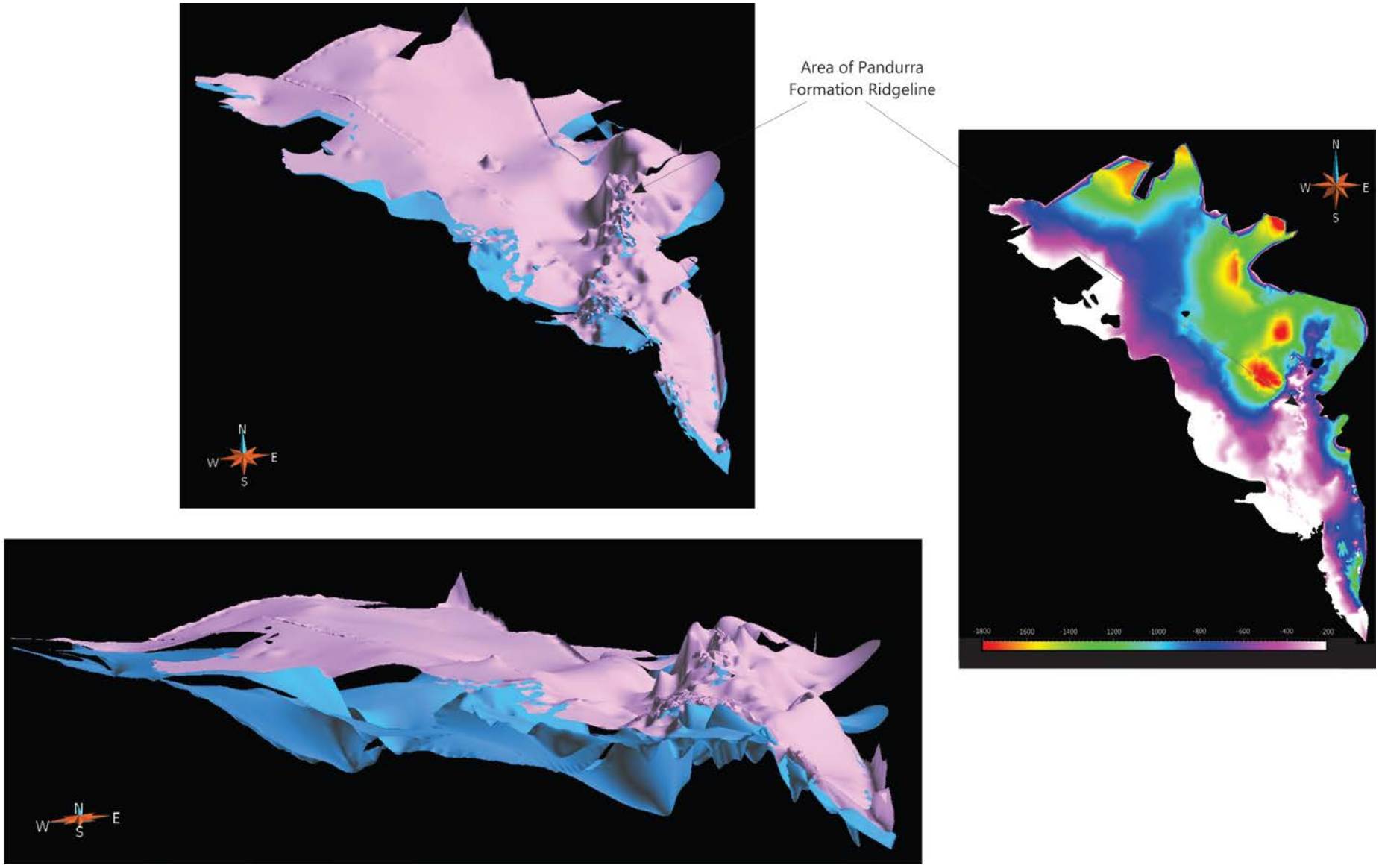

Figure 13: *Basal (blue) and Upper (pink) Pandurra Formation surfaces. Top left: inclined plan view looking north. Bottom Left: cross section view looking north-east. Both left views at 50x vertical exaggeration to enable better visualisation of features. The Pandurra Formation Ridgeline is visible on the eastern side of the basin in the top image. Right, Pandurra Formation thickness as calculated from the two Pandurra Formation Surfaces, thickness colour ramp in metres. Thickness image clipped to the Cariewerloo Basin Modified Polygon.*

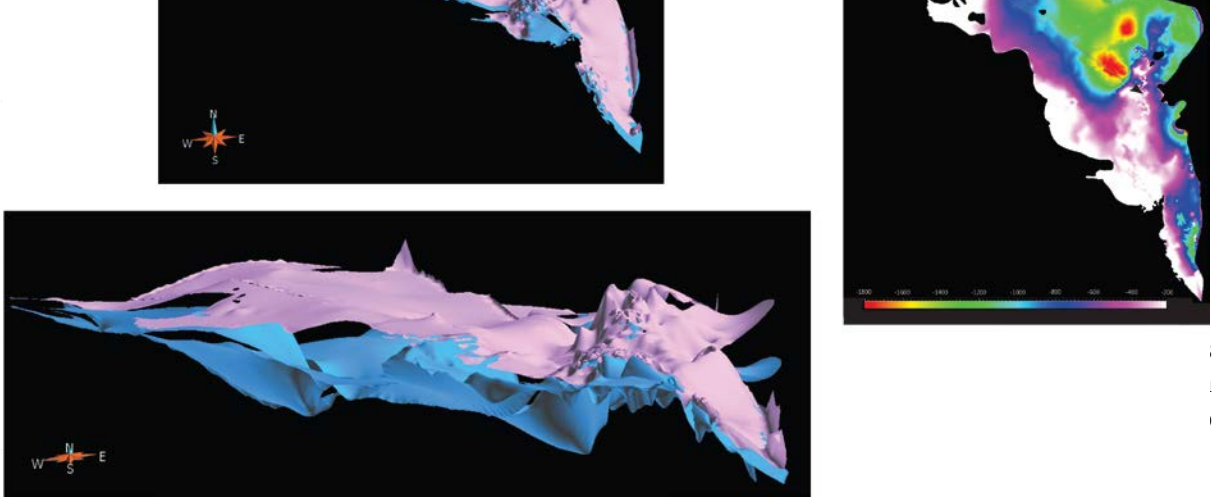

rk within, and also provide information in their own right as they illustrate the topography and thickness of the Pandurra Formation. They also enable volumetric calculations; for example: the Pandurra Formation region occupies approximately 16,100 km^3. Further calculation within these regions are beyond the scope of this study, but would enable the volume occupied by a particular property range to be calculated using statements such as 'volume of rock with U>5 ppm within the Pandurra Formation' which would be useful for exploration and resource estimation. The Cover and Pandurra voxet regions are shown from side on (i.e. not a cross-section) in Figure 14. The highly variable thickness of the Pandurra and Cover are clearly visible, as are the geological and topographic features that may be important in terms of surficial fluid flow penetration, fluid pooling and associated late-stage alteration process. Basement highs are also visible in the lower Pandurra region topography.

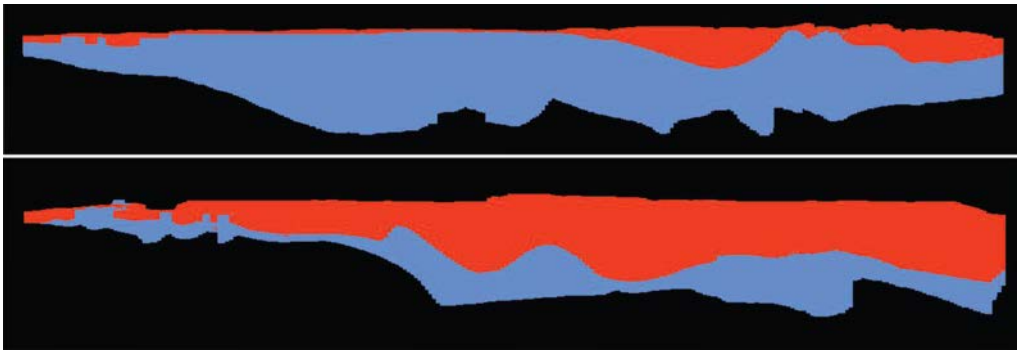

Figure 14: *Cover (orange) and Pandurra (blue) regions of voxet as seen from the south (top) and the west view points (bottom). Vertical exaggeration 20x, voxet regions side view.*

A more detailed view of the Pandurra voxet volume is shown in Figure 15. It highlights the highly localised variation in Pandurra Formation thickness as a result of syn- and post-depositional faulting, and subsequent erosion. The strongly-faulted eastern Cariewerloo Basin margin with thick Pandurra Formation and the thin onlapping relationship with underlying lithologies on the western margin are clearly visible.

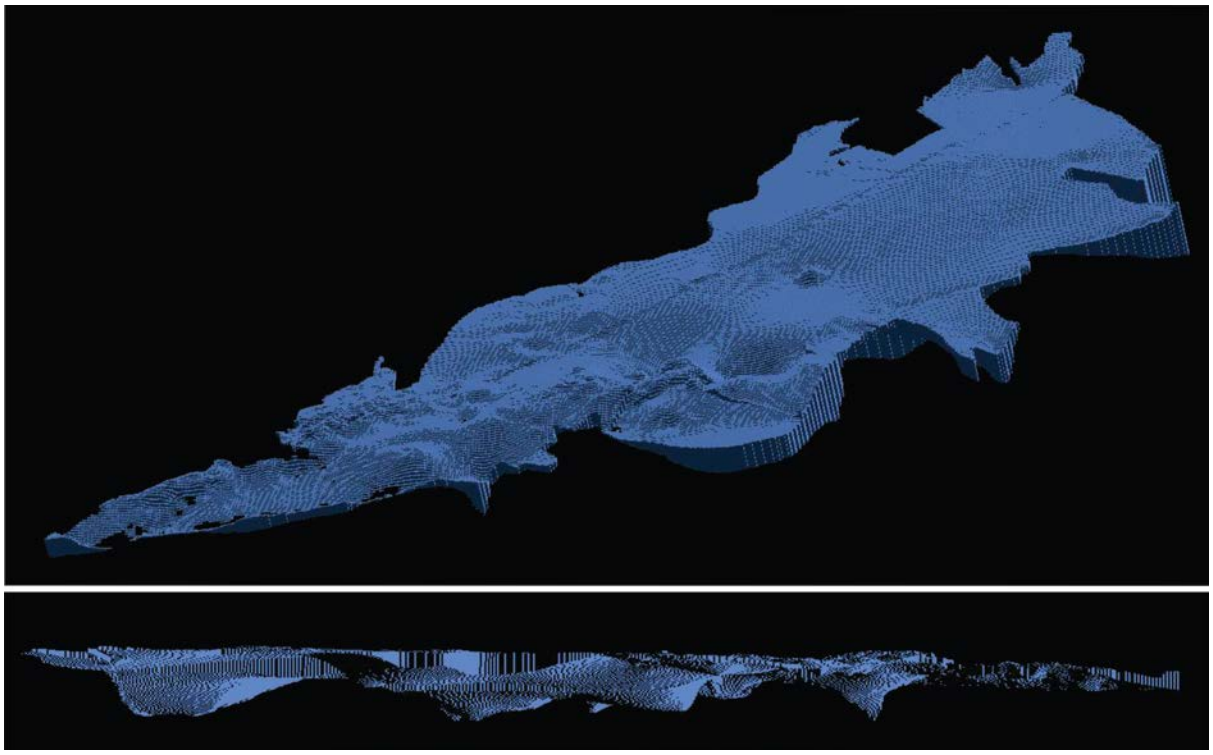

Figure 15: *The Pandurra Formation volume as rendered from the Upper and Basal Pandurra Formation surfaces. Top view, inclined plan view looking north-west. Bottom view, cross section view looking east. Both views have 20x vertical exaggeration.*

On closer inspection in GOCAD, the voxet surface reveals major basement lows and subsequent significant thicknesses of Pandurra Formation west of Mt Gunson/Emmie Bluff, south of the Acropolis Prospect, near Prominent Hill, and on the peninsula-like protrusion of the eastern northern basin margin near RCDD04TI008.

A complex ridge of basement highs extends from north of Emmie Bluff (see Figure 1), south through the main body of the eastern basin, and emerges at the southern margin of the basin, just east of Mt Laura (see Figure 16 below). This ridge occupies quite a narrow zone in the north, which broadens out to a zone approximately 50 km wide at the basin margin near Cariewerloo Station, after which only the eastern margin of the ridge is within the current basin margin. The relative elevation of the ridgeline decreases towards the southern basin margin. The eastern margin of the proposed 'Pandurra Formation Ridgeline' is nearly coincident with the Ridgeline East trend line identified in the geochemistry and Pandurra Formation surfaces topography from this study. This ridgeline can also be seen to a lesser extent in the Pandurra Formation thickness map in Figure 13. The Upper Pandurra Formation surface, the newly proposed Ridgeline East Trend Line, and the topographically-defined Ridgeline West Trend Line are shown in Figure 16. While the trend lines have been drawn as simple linear trend lines at this stage, the western margin of the Pandurra Formation Ridgeline zone is much more complex in detail. In contrast, the eastern margin as defined geochemically is remarkably linear, although it does pass just to the west of the basement high north of Emmie Bluff as currently drawn, and so could be interpreted in more detail to include minor segmented deviations in the ridgeline margin to fit the observed basement highs even more closely (as likely influenced by localised faulting).

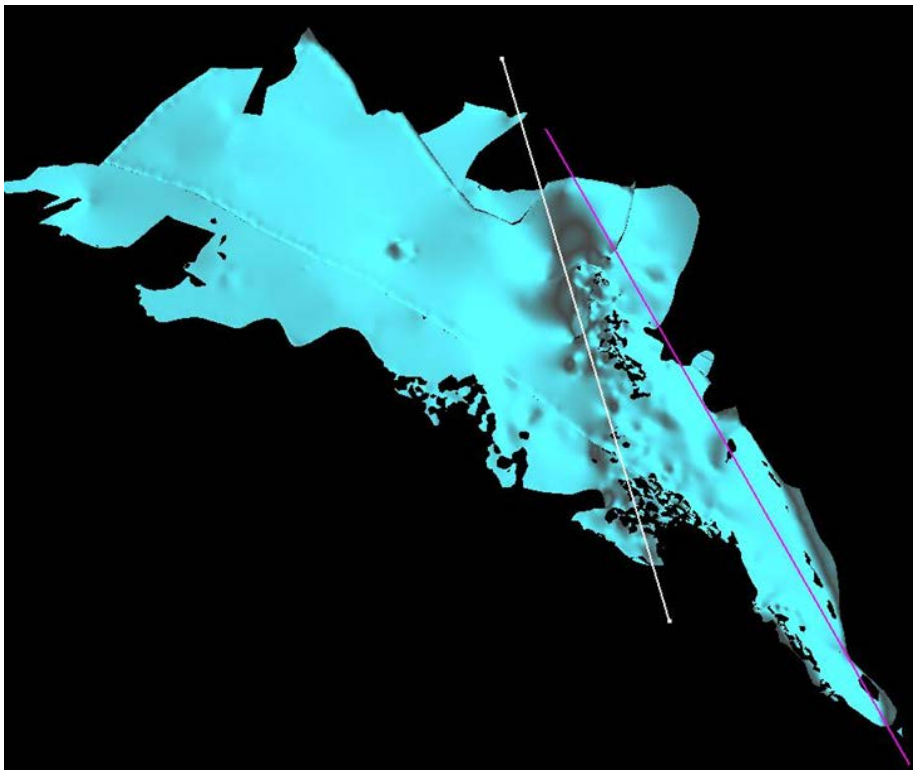

Figure 16: *Inclined plan view of the Upper Pandurra Formation surface with proposed Pandurra Formation Ridgeline margins. The Ridgeline East Trend Line (pink), and the Ridgeline West Trend Line (white) are shown. Vertical exaggeration 20x, inclined plan view towards the northeast.*

The same limitations that apply to the surfaces apply to the voxet. The only additional limitation is the unavoidable issue of voxet resolution affecting Pandurra Formation geometry. The resolution chosen for the voxet is quite high having a cell size of 1 km by 1 km by 10 m. However, even this resolution is not enough to do a particularly smooth rendering of the complexly curved Pandurra Formation surfaces. In spite of these aesthetic draw-backs, the high resolution of the voxet is more than adequate to resolve reasonably high-level grain size and geochemical detail. The interpolation of unevenly distributed data at this resolution has generated some localised artefacts which are best viewed in GOCAD.

Grain size interpolated voxet

A selection of GOCAD sections showing the interpolated grainsize voxet are shown in Figure 17. GOCAD section numbers refer to planar horizontal slices cut through the voxet. The section numbers do not indicate actual depth, but rather the sequential numbering of voxet sections from top to bottom. Smaller section numbers indicate shallower depths.

Isosurfaces

To aid visualisation, and to enable further interrogation of the geochemical voxet by end-users, isosurfaces were generated for each grain size classification subdivision. A selection of the isosurfaces generated are shown in Figure 18. These were generated as tools for identifying potential fluid-flow pathways associated with primary porosity. Used in conjunction with the ‘proximity to fault’ voxet properties, these isosurfaces will enable the first-pass assessment of both primary and secondary porosity around the faults used to generate the voxet.

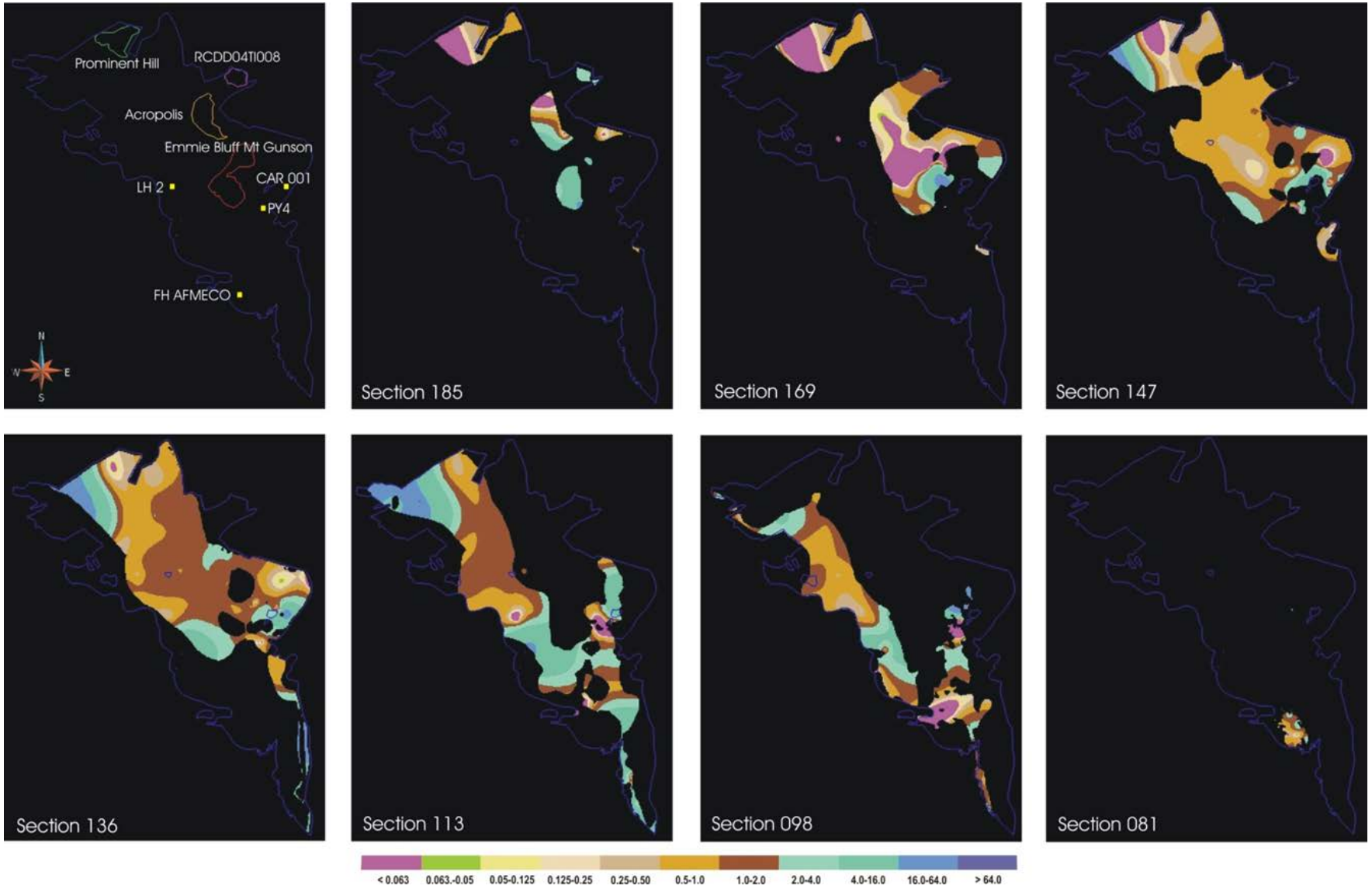

Figure 17: *Interpolated grain size voxet plane sections as described in the text from top left to bottom right of the page. The four major depocentres and drillholes well-known drillholes are shown in the top left image. The grain size classification key in mm is shown below the images. Cariewerloo Basin Polygon Modified curve shown for reference.*

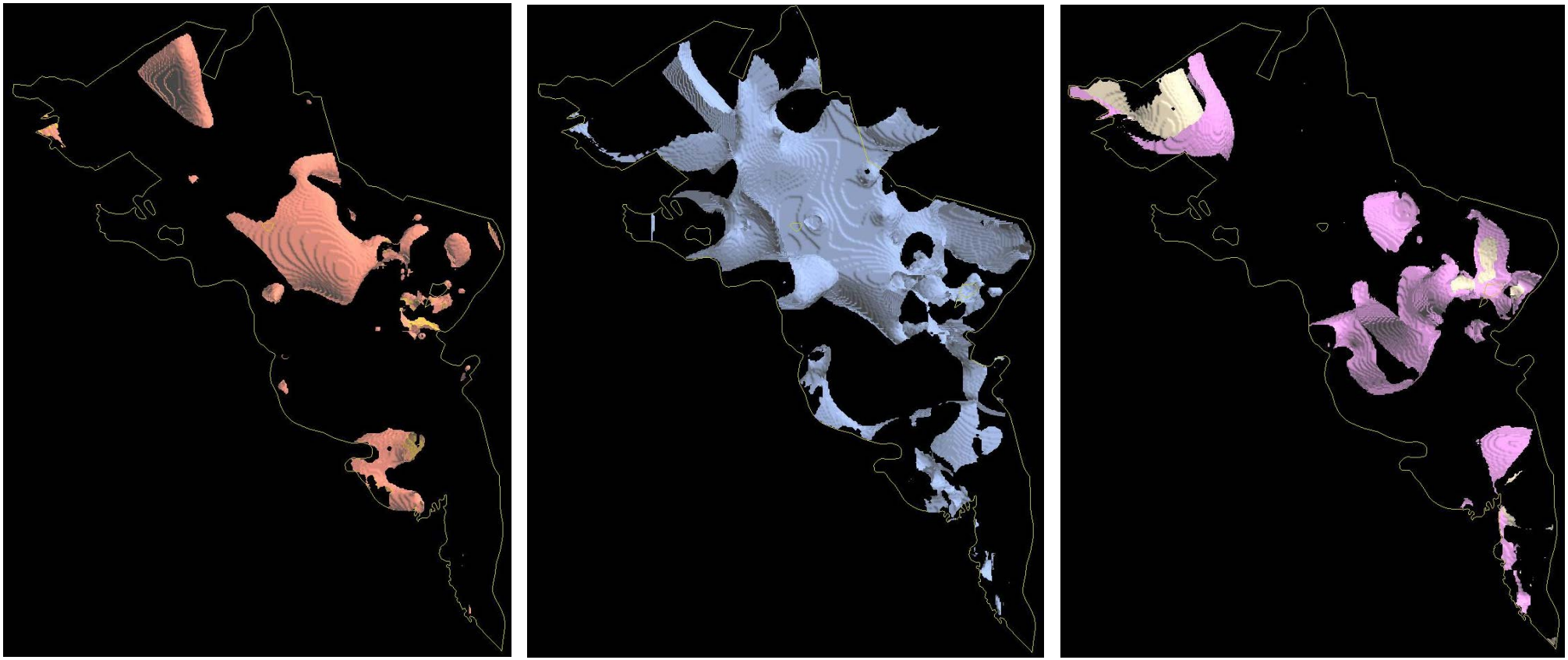

Figure 18: *Selected Pandurra Formation Grainsize Isosurfaces in plan view. From left to right: 0.063 mm (yellow) and 0.05 mm (orange) isosurfaces; 1 mm blue isosurface; 4 mm (pink) and 16 mm (white) isosurfaces. As the isosurfaces are defined in 3D space by all the components of the voxet, black appears where the other isosurfaces, Pandurra Surfaces, and the DEM would usually enclose the rest of the isosurface.*

References

Bacchin, M., Milligan, P.R., Wynne, P. and Tracey, R. (2008). Gravity Anomaly Map of the Australian Region (Third Edition), [Digital Dataset], 1:5,000,000 scale, Geoscience Australia,

Cowley, W. M. (1991). *The Pandurra Formation*. Department of Mines and Energy South Australia, Report Book 91/7.

Cruickshank, B.I. and Pyke, J.G. (1993). Analytical Methods Used in Minerals and Land Uses Program's Geochemical Laboratory. *Australian Geological Survey Organisation*, 26, 26pp.

Gallant, J.C., Dowling, T.I., Read, A.M., Wilson, N., Tickle, P. and Inskeep, C. (2011). 1 second SRTM Derived Digital Elevation Model vs. 1.0. Geoscience Australia, Commonwealth of Australia, Canberra. ANZCW0103013355.

Mallet, J.L., (1992a). Discrete smooth interpolation in geometric modelling. *Computer Aided Design*, 24, 178–191.

Mallet, J.L., (1992b). GOCAD: A computer aided design program for geological applications. *In*: Turner, A.K., (editor). *Three-dimensional Modelling with Geoscientific Information Systems.* Kluwer Academic Publishers, Netherlands, 123–141.

Mason, M.G. (1980). Island Lagoon, EL301. Sixth Quarterly Report, 23rd June – 22nd September 1978, for Australian Selection (Pty) Ltd. *South Australia Department of Mines and Energy*, Open File Envelope 2996, 129–204.

Milligan, P.R., Franklin, R., Minty, B.R.S, Richardson, L.M. and Percival, P.J., (2010). Magnetic Anomaly Map of Australia (Fifth edition), [Digital Dataset], 100 m pixels, Geoscience Australia, Commonwealth of Australia, Canberra.

Minty, B.R.S., Franklin, R., Milligan, P.R., Richardson, L.M. and Wilford, J., (2010). Radiometric Map of Australia (Second Edition), [Digital Dataset], 100 m pixels, Geoscience Australia, Commonwealth of Australia, Canberra.

Norrish, K. and Hutton, J.T. (1969). An accurate X-Ray spectrographic method for the analysis of a wide range of geological samples. *Geochimica et Cosmochimia Acta*, 33, 431–453.

SARIG, 1:100,000 scale Surface Geology polygons, ANZCW0703002399. Downloaded 2009. https://sarig.pir.sa.gov.au.

SARIG, Cariewerloo Basin Polygon, Middle – Late Mesoproterozoic Mineral Geological Province. Downloaded 2011. http://www.minerals.dmitre.sa.gov.au/sarig/metadata/geology/mineral_geological_provinces/middle_to_late_mesoproterozoic

Shapiro, L. and Brannock, W.W. (1962). Rapid analysis of silicate, carbonate, and phosphate rocks. *U.S. Geological Survey Bulletin* I, l 44A, 56.

Tonkin, D. G. (1978). Report on deep stratigraphic drill hole EC 21, Gunson, EL543. Appendix 1, Report EMR 42/80, for CSR Limited – Minerals Division, Exploration Group. *South Australia Department of Mines and Energy,* Open File Envelope 3703. 432–525.

van der Wielen, S. and Korsch, R.J. (eds.) (2005). 3D architecture and predictive mineral system analysis of the Central Lachlan subprovince and Cobar Basin, New South Wales: Final report of the pmd*CRC T11 project. Geoscience Australia.

van der Wielen, S. et al., Kirkby, A., Britt, A., Nicoll, M., Lewis, B., English, P., Chopping, R. and Skirrow. (in prep.). An integrated, multiuse 3D map for the greater Eromanga Basin, Australia. *Geoscience Australia Record*.

Wentworth, C.K. (1922). A scale of grade and class terms for clastic sediments, *Geology*, 30, 377–392.

Wilson, T., Bosman, S., Heath, P., Gouthas, G., Cowley, W., Mauger, A., Gordon, G., Baker, A., Dhu, T., Fairclough, M., Delaney, G., Roach, I., Huchison, D. and Costelloe, M. (2011). Cariewerloo Basin Unconformity-Related Uranium Project: Data Release April 2011. Geological Survey of South Australia, Department for Manufacturing, Innovation, Trade, Resources and Energy (formerly Primary Industries and Resources SA). DVD.